Stromatolite records of environmental change in perennially ice-covered Lake Joyce, McMurdo Dry Valleys, Antarctica

Mackey TJ[1,2], Sumner DY[2], Hawes I[3], Leidman SZ[2,4], Andersen DT[5], Jungblut AD[6]
[1] Department of Earth, Atmospheric and Planetary Sciences, Massachusetts Institute of Technology, 77 Massachusetts Avenue, Cambridge, Massachusetts 02139, USA, tjmackey@mit.edu, 1-617-452-2784, ORCID 0000-0001-6377-3797
[2] Department of Earth and Planetary Sciences, University of California–Davis, 1 Shields Avenue, Davis, California 95616, USA
[3] Tauranga Coastal Research Laboratory, University of Waikato, 58 Cross Road, Tauranga 3110, New Zealand
[4] Department of Geography, Rutgers, The State University of New Jersey, Piscataway, NJ 08854, USA
[5] Carl Sagan Center for the Study of Life in the Universe, SETI Institute, Mountain View, CA 94043, USA
[6]Department of Life Sciences, The Natural History Museum, Cromwell Road, London SW7 5BD, UK

ABSTRACT

Calcite-rich columnar stromatolites grew in perennially ice-covered Lake Joyce in the McMurdo Dry Valleys, Antarctica, during a period of environmental change associated with rising lake level. Stromatolite calcite contains carbon and oxygen isotope records of changes to microbial activity in response to variable light environments and water chemistry through time. The stromatolites grew synchronously with correlative calcite zones. The innermost (oldest) calcite zone has a wide range of $\delta^{13}C_{calcite}$ values consistent with variable photosynthetic effects on local DIC $^{13}C/^{12}C$. Subsequent calcite zones preserve a progressive enrichment in $\delta^{13}C_{calcite}$ values of approximately +2.6‰ through time, with $\delta^{13}C_{calcite}$ values becoming less variable. This enrichment likely records the removal of ^{12}C by photosynthesis from the DIC reservoir over decades, with photosynthetic effects decreasing as light levels became lower and more consistent through time. Mean $\delta^{18}O_{calcite}$ values of the innermost calcified zone were at least 1‰ lower than those of the other calcified zones (t-test p-level <0.001). The significant difference in $\delta^{18}O_{calcite}$ values between the innermost and other calcified zones could be a product of mixing source waters with different isotopic values associated with the initiation of lake stratification associated with rising lake level. Overall, Lake Joyce stromatolites record significant lateral variability in relative photosynthetic rate and long-lived lake water stratification with microbial modification of the DIC pool. Such processes provide criteria for interpreting microbial activity within polar paleolake deposits and may shed light on variability in lake environments associated with changing climate in the McMurdo Dry Valleys.

Key words: Antarctica; stromatolite; microbial mat; carbonate; isotopes

ACKNOWLEDGEMENTS

This project was supported by funding from the National Aeronautics and Space Administration Astrobiology: Exobiology and Evolutionary Biology Program (NNX08AO19G and NNX13AI60G). Sample analyses were further supported by funding through the UC Davis Earth and Planetary Sciences Durrell Funds. Sample freeze drying and preparation was courtesy of T. Doane at UC Davis, petrography was supported by F. Corsetti at USC, and the manuscript was significantly improved through conversation with H. Spero. Data sets in this project relied on the shared work of the field teams for United States Antarctic Program events G-441 and G-063.

1 INTRODUCTION

Polar environments are particularly sensitive to changes in climate, and even small changes in absolute temperature can dramatically affect the availability of liquid water in catchments dominated by ice or snow pack (e.g. Quesada et al., 1996; Fountain et al., 1999). Such variations in regional hydrology are important in the polar deserts of Antarctica (Doran et al., 2008; Gooseff et al., 2011). In the McMurdo Dry Valleys (MDV), the largest ice-free region of Antarctica, meltwater streams, wetted soils, ponds, and lakes with 3-7 m of perennial ice-cover (Chinn, 1993; Gooseff et al., 2011) serve as oases for photosynthetic primary productivity (Quesada et al., 2008). With changing regional MDV climate, excess meltwater influx relative to evaporation or ice ablation has led to rising water levels in perennially ice-covered, closed-basin (endorheic) lakes (Chinn, 1993; Hawes et al., 2011; Castendyk et al., 2016). Expansion and contraction of such lakes through MDV history thus provides a record of regional hydrology crucial to interpretation of Antarctica's sensitivity to climate change and the availability of aqueous habitats for primary productivity in an otherwise icy environment (Quesada et al., 2008; Convey et al., 2014).

The history of MDV endorheic lake level is preserved in both the stratified water column and sediments of perennially ice-covered lakes. Water columns typically contain steep gradients in salinity (e.g. Spigel and Priscu, 1998), where deep, salty water generated by freeze-concentration under stable or falling lake levels are overlain by lenses of fresher water that form during episodes of lake level rise (Chinn, 1993; Green and Lyons, 2009). Salinity stratification is stable in MDV lakes over hundreds of years because ice cover restricts mixing by wind-driven waves or currents (e.g. Wilson, 1964; Matsubaya et al., 1979; Hall et al., 2017). Deep lake brines indicate that lakes throughout the MDV contracted to a minimum approximately 1000–1200 years ago and have filled since (Lyons et al., 1998). On longer time scales, sediments from MDV lakes provide evidence for larger lake level changes. Paleolake deposits range from perched deltas and paleoshorelines 10s to 100s of m above current lake levels during the last glacial maximum (summarized in Doran et al., 1994; further discussion in Brockheim and McLeod, 2013) to deep basin evaporates that represent repeated contraction of lakes over tens of thousands of years (Gumbly, 1975; Clayton-Greene et al., 1988). Independent evidence for perennial ice cover in these paleolake deposits include sand mounds (Squyres et al., 1991; Andersen et al., 1993) and transport and sorting of sediments by the ice cover "conveyor belt" (see Hendy et al., 2000 for discussion of the conveyor belt

model). The variability in meltwater influx necessary to explain these lake environments between climate states highlights the sensitivity of MDV hydrology to local conditions (e.g. Castendyk et al., 2016).

Sediment deposits from recent MDV lakes and paleolakes also include carbonates, which may preserve additional information about the response of lakes to changing regional climate and their aqueous habitats (e.g. Lawrence and Hendy, 1985). Most carbonates in MDV lakes precipitate within benthic microbial mats that coat the lake bottom, with the extent of precipitation ranging from discrete crystals disseminated within the microbial mats to mm-thick carbonate layers forming modern microbialites (Wharton et al., 1982; Wharton et al., 1983; Sutherland and Hawes, 2009; Hawes et al., 2011). Similar carbonates in MDV paleolake deposits consist of plates associated with preserved microbial mat material (Hendy et al., 1979; Clayton-Greene et al., 1988; Doran et al., 2008). In this study, we examine the stable isotope geochemistry of recent microbial carbonates from Lake Joyce to tie microbial activity and changing environmental conditions to lake level rise. These paired records may provide a window into interpretation of paleolake deposits to constrain the relationship between changing regional hydrology and ecosystems in perennially ice covered lakes.

2 BACKGROUND

2.1 Lake Joyce

Lake Joyce (77.72°S, 161.62°E) is located in Pearse Valley of the MDV and abuts Taylor Glacier, a spur of the Ferrar ice stream sourced from the Antarctic polar plateau (Fig. 1). Meltwater enters Lake Joyce from both Taylor Glacier and surrounding alpine glacier streams (Green et al., 1988), but the lake has no outflow. This region has a mean annual temperature of approximately -18 °C (Doran et al., 2002; data from 1993-2000 at adjacent Lake Bonney, Taylor Valley), which limits meltwater production to austral summer periods when air temperatures are warm or direct solar heating melts ice. As a result, the influx of meltwater is very sensitive to small changes in summer conditions.

The surface of Lake Joyce is approximately 1 km^2 and comprises a 4-7 m-thick ice cover overlying a density stratified water body (Hall, 1973; Spigel and Priscu, 1998). Temperature contributes little to the density stratification, with a maximum temperature of 1.1 °C (Shacat et al., 2004), whereas salinity increases with depth. Salinity increases across two density gradients centered on 13 and 19 m

depth, respectively (Spigel and Priscu, 1998; Hawes et al., 2011), with deep water Na and Cl concentrations exceeding 40 mM (Shacat et al., 2004). Salinity-stratified layers in Lake Joyce formed with freshwater influx following periods of falling or stable lake levels, when freezing excluded solutes at the underside of the ice cover and increased lake salinity (e.g. Chinn, 1993). Meltwater influx into Lake Joyce has been increasing the thickness of the upper freshwater lens, and hence lake level, by approximately 0.2 m y^{-1} since regular observations began in 1972 (Hawes et al., 2011). Deeper water salinity stratification has been stable since the first observations in 1972 (Gumbly, 1975; Hawes et al., 2011), and radiocarbon dates of approximately 2500 y B.P. suggest that waters below the pycnocline have been isolated from shallower waters for hundreds to thousands of years (Hendy and Hall, 2006).

Stratified lake water in Lake Joyce is also associated with changes in isotope composition. $\delta^{18}O_{H2O}$ values decrease with depth through the stratified water column. Water at 10.5 m depth has a maximum $\delta^{18}O_{H2O}$ value of -38.2‰, and the value decreases to -40.3‰ at 22.5 m and then to a minimum of -42.9‰ at 36.5 m (data from www.mcmlter.org for samples collected in 2008, depths adjusted to 2014 lake levels). The negative correlation between $\delta^{18}O_{H2O}$ values and salinity is consistent with freeze concentration of lake waters, given typical fractionation of approximately +3‰ between ice and liquid water (O'Neil, 1968; Suzuoki and Kimura, 1973). For discussion of $\delta^{18}O_{H2O}$ values for water sources contributing to Lake Joyce, see supplemental materials.

2.3 Irradiance

The Lake Joyce ice cover affects transmission of photosynthetically active radiation (PAR). PAR transmitted through the ice cover varies by an order of magnitude laterally in Lake Joyce and other lakes with similar ice cover (Hawes et al., 2011; Hawes et al., 2016), likely due to long-lived pockets of sediment in the ice cover and differences in ice opacity (McKay et al., 1994; Howard-Williams, 1998). In Lake Joyce, 0.37 to 4.3% of incident irradiance was transmitted through the ice cover in 2009 and 2010, and variability in PAR decreased with depth as heterogeneities in ice cover transmission were averaged over a greater area (Hawes et al., 2011; Mackey et al., 2017). Irradiance decreases with a vertical attenuation coefficient of 0.12 m^{-1} (Hawes et al., 2011).

2.4 Microbial ecosystem

Benthic microbial mat communities are the source of most biomass accumulation with water column primary productivity low in most modern MDV lakes where comparisons have been made (Moorhead et al., 2005). Net photosynthetic biomass accumulation continued down to approximately 1 µmol photons m^{-2} s^{-1} in several perennially ice-covered MDV lakes (Hawes and Schwarz, 1999; Hawes et al., 2014), and this irradiance limit is reached at approximately 13-16 m depth in Lake Joyce (Hawes et al., 2011). Net respiration occurs to greater depths, and induces a transition from the hyperoxic freshwater lens of Lake Joyce to deeper water anoxia (Shacat et al., 2004; Hawes et al., 2011). The balance of photosynthesis to respiration also affects the DIC pool $\delta^{13}C_{DIC}$ values. In the euphotic zone, net photosynthesis preferentially sequesters ^{12}C into organic matter, leaving the ambient DIC pool relatively enriched in ^{13}C (Neumann et al., 2004; Knoepfle et al., 2009). Conversely, net oxidation of organic carbon at greater depths reduces the ratio of $^{13}C/^{12}C$ in the DIC (Neumann et al., 2004; Knoepfle et al., 2009). In Lake Joyce, $\delta^{13}C_{DIC}$ values of the shallowest lake layer exceeded +10‰ in 1997 due to photosynthesis in the euphotic zone and decreased below -1‰ deeper than 24 m due to respiration (Neumann et al., 2004; see supplemental materials for more discussion).

Benthic mat biomass is largely produced by filamentous cyanobacteria (Wharton et al., 1983; Zhang et al., 2015). Pigmented photosynthetic microbial mats covered the bottom of Lake Joyce above the PAR limit of 13-16 m, but at greater depths, microbial mats were coated with sediments and pigment abundances declined relative to their degradation products, consistent with the dominance of respiration below the PAR limit (Hawes et al., 2011).

2.5 Stromatolites

Calcified photosynthetically active and degraded microbial mats are abundant in Lake Joyce to a depth of 23 m (Wharton et al., 1983; Hawes et al., 2011; Mackey et al., 2015). The largest microbial structures are dm-scale branched columnar stromatolites present at approximately 22-23 m depth (Fig.2). Stromatolites layered with varied proportions of calcite, organic matter, and sediment (Hawes et al., 2011; Mackey et al., 2015). Calcite layers are made up of isolated to intergrown, equant to elongate crystals, and fibrous crystals forming either isopachous crusts or botryoids up to 2 mm thick (Mackey et al., 2015). All calcite textures contain filamentous microfossils interpreted as entombed cyanobacteria, and some botryoidal layers locally affected sedimentation by causing relief at the mat surface. Taken together, these

observations support the interpretation that calcite precipitated close to the surface of cyanobacterial mats (Mackey et al., 2015).

Mackey et al (2015) documented that the stromatolites grew during an interval of lake level rise, and the innermost layers of stromatolites are consistent with initiation of growth at lower lake levels than were first documented in 1972 (Hawes et al., 2011). Ambient lake water was supersaturated with respect to calcite, demonstrated during the later stages of stromatolite growth by a log saturation index of 1.0 at 23 m in 1981 (Green et al., 1988; depth adjusted to 2014 lake level). pH, Ca, and DIC were comparable between measurements in 1981 and repeat measurements at 21 and 23 m in 2001 (Shacat et al., 2004). Despite the similarity in carbonate chemistry through at least two decades of stromatolite growth, changes in lake level resulted in large changes in photosynthetic environment. By 2009, lake levels had risen to the point that stromatolites lacked evidence for net photosynthetic activity (Hawes et al., 2011). In this study, we use stromatolite calcite isotopic records to reconstruct microbial activity under changing environmental conditions in Lake Joyce.

3 METHODS

Collection of intact benthic stromatolite samples and *in situ* measurements were performed by scuba divers (after Andersen, 2007). Dive holes were melted through the ice cover of Lake Joyce in November 2009, October to November 2010, and November 2014 (Fig. 1), providing access to the lake water and stromatolites.

3.1 pH microelectrode measurements

Divers deployed a micromanipulator at 12 m depth to measure pH microelectrode profiles in microbial mats. The microelectrode data were logged using a Unisense (Aarhus, Denmark) UWM underwater meter/datalogger in mV mode fitted with a Unisense p50 pH microsensor with a 50 µm tip diameter. The microelectrode was calibrated at ambient temperature with NBS reference standard buffers at pH 4, 7, and 10. To characterize pH with depth in the mats, divers used a micromanipulator to lower the microelectrode from the water column into the mat in 0.5 mm increments. The location of the microbial

mat surface was estimated by the diver and confirmed by analysis of the pH profile. The pH was measured at a single point in the diffusive boundary layer across a diurnal cycle 23-24 November 2014.

3.2 Stromatolite and mat analyses

Columnar stromatolites were collected from depths of 21.8 to 23.0 m at two sites separated by approximately 350 m (Table 1) in November 2009 and 2010. In 2010, a sample of microbial mat with bulbous pinnacles (sensu Hawes et al., 2011) was also collected at 16.6 m. To collect samples, divers placed acrylic tubes over intact columnar stromatolites and microbial mat, pushed the tubes into the sediment, capped the tops of tubes, removed the tubes, and capped the bottoms (Fig. 1). The depth of sampling sites was resolved to ~0.3 m based on dive computers, but the depth of one stromatolite collected in 2009 is unknown within 1.2 m (Table 1). Cores and mat samples were frozen on site with dry ice (2010) or refrigerated at <4 °C for up to 23 days on site before being transported back to McMurdo for freezing (2009). Stromatolites were kept frozen throughout transport and storage to keep them intact.

3.2.1 Stromatolite characterization

Ten frozen stromatolites were x-ray CT scanned at the UC Davis Center for Molecular and Genomic Imaging, using the methodology of Mackey et al. (2015). In brief, samples were scanned on a Siemens Preclinical Solutions Inveon CT scanner, and 3D computed density maps were reconstructed with the COne Beam Reconstruction Algorithm, FieldKamp algorithm and beam hardening correction. Resulting reconstructions were down sampled 4× giving 196×196×196 µm voxels.
Stromatolite reconstructions were visualized using VRUI 3DVisualizer in the UC Davis KeckCAVES (after Stevens et al., 2011; Kreylos, 2008; www.keckcaves.org). 3D investigation provided context for targeted subsampling of frozen stromatolites. Segments of 7 frozen stromatolites were cut with a band saw into approximately 1 cm horizontal slices, which were subsequently thawed or freeze dried. Slices from 6 stromatolites were impregnated with EpoFix and cut into 80 µm thick sections for optical petrography and calcite $\delta^{13}C$ and $\delta^{18}O$ isotopic analyses.

3.2.2 Calcite ^{13}C isotopic analysis

Thawed and freeze dried stromatolites were dissected and microdrilled for calcite isotopic analyses. Dissected calcite layers approximately 0.5 to 1 mm thick were removed from 6 stromatolites and homogenized by grinding in a mortar and pestle. Layers from 5 stromatolites were subsampled by

microdrilling thick sections using a Merchantek Micromill with programmed rasters that were approximately 100 µm wide and 40-50 µm deep. Microdrilled rasters were visually inspected by optical petrography for incorporation of EpoFix epoxy and the degree to which drilled rasters followed individual laminae within stromatolite layers. No samples contained significant epoxy, and all followed planned drill paths.

Powdered calcite samples from stromatolite layers were analyzed for $\delta^{13}C_{calcite}$ and $\delta^{18}O_{calcite}$ at the UC Davis Stable Isotope Lab. All samples were heated to 375 °C *in vacuo* for 30 minutes prior to analysis. Samples were analyzed via either 1) a GV Instruments IsoPrime dual inlet mass spectrometer interfaced to a Gilson Multicarb Autosampler or 2) a GVI Optima Stable Isotope Ratio Mass Spectrometer with a common acid bath (see supplemental materials for details of isotopic analysis). $\delta^{13}C_{calcite}$ and $\delta^{18}O_{calcite}$ values are reported relative to VPDB.

3.2.3 Petrographic analysis and correlation

At a coarse scale, stromatolite layers were correlated by repeated patterns of petrographic textures. The thicknesses of correlated calcite layers varied within and between stromatolites, so layer thicknesses were normalized to create a shared axis of "normalized distance from stromatolite center" for presentation of carbonate isotope geochemical data. Layer thicknesses were averaged along 12 radial transects in thick sections of 3 representative stromatolites. Where stromatolite layers were absent in a transect, layer thickness was not measured. Correlations within the acicular layer of calcite zone 1 were further refined by comparison of patterns in relative laminae thickness in stromatolites 1, 2 and 3. The thickness of each unit was measured in five radial transects through the acicular calcite layer and divided by the full layer thickness to give the fraction of the stromatolite comprising each unit. Where stromatolite layers were subsampled, the proportion of the layer covered by the microdrill raster was measured, and the drill width was scaled to the mean layer thickness and positioned at the proper relative radius in relevant plots.

3.2.4 Biomass ^{13}C isotopic analysis

Sections of one stromatolite from 22.1 m and one bulbous pinnacle from 16.6 m were cut from frozen samples and thawed for organic carbon $\delta^{13}C$ analysis. The organic-rich portions of the stromatolite and bulbous pinnacle subsamples were physically separated from the underlying calcite layers, acidified three times with 0.25 M HCl to remove calcite, rinsed in MilliQ water, and dried at 40°C. Dried samples

were transferred to silver capsules and subsequently analyzed at the UC Davis Stable Isotope Facility with a PDZ Europa ANCA-GSL elemental analyzer connected to a PDZ Europa 20-20 isotope ratio mass spectrometer (Sercon Ltd., Cheshire, UK; see supplemental materials for details of isotopic analysis). $\delta^{13}C_{org}$ values are reported relative to VPDB.

3.3 Water column measurements and water samples

Measurements of lake conductivity were made through the water column over the deepest known part of Lake Joyce (Fig. S1**)** using a YSI 6600 Sonde (after Hawes et al., 2011). Lake level rose during this study, and changes in depth were determined by aligning steep gradients in conductivity, which have been stable over decades of observation (Gumbley, 1975; Green et al., 1988; Shacat et al., 2004; Hawes et al., 2011). All depths reported in this manuscript were converted to equivalent depths in November 2014.

Meltwater samples from a stream draining both the Catspaw and Taylor glaciers were collected 24-hours apart during early season melt on 07 and 08 December 2015 (stream J5 of Green et al., 1988; Fig. 1). Water column samples were collected in a 2.2 L General Oceanics Niskin bottle at 22 m depth from the same site as conductivity measurements. Water samples for $\delta^{13}C_{H20}$ were preserved by injecting 5 mL into prepared 12 mL Exetainers containing 1 mL of 85% H_3PO_4 under He head space. Samples collected for $\delta^{18}O_{H20}$ analysis were collected in 125 mL Nalgene bottles. All samples were refrigerated during transport to UC Davis. Water samples were analyzed at the UC Davis Stable Isotope Facility, where Exetainers were flushed with a He carrier gas to pass sample CO_2 through a Poroplot Q GC column before entering a GasBench II interfaced to a Thermo Scientific Delta V Plus IRMS. Analysis of all water samples for $\delta^{18}O_{H20}$ was made on a Los Gatos Research, Inc. Laser Water Isotope Analyzer V2 (see supplemental materials for details of analytical methods). All $\delta^{18}O_{H20}$ values are reported relative to VSMOW, and $\delta^{18}O_{calcite}$ values are reported relative to VPDB.

3.4 Bathymetric model

The bathymetry of Lake Joyce was reconstructed using diverse data sets. 18 soundings through holes drilled in the ice cover came from Hendy et al. (1973), adjusted to account for lake level rise, and 57 new soundings were made in October-December 2014. Shallow bathymetry of recently submerged terrain (<3.7 m depth in 2014) was taken from a 2001 USGS LIDAR-based DEM (Schenk et al., 2004), and shoreline GPS coordinates were collected by handheld GPS units in 2010 and 2014. Shorelines in 1947,

1961, 1970, 1983 and 1993 were determined from trimetrogon aerial (TMA) photographs archived at the Polar Geospatial Center. Each image was georeferenced to the 2001 USGS DEM using a minimum of 6 ground control points. Georeferenced photographs were ranked by ground control point RMS error, and in cases of conflicting data points, those with the lowest RMS error were used. Aerial photograph shorelines were downsampled into depth sounding points to extrapolate bathymetry from better-constrained regions in the lake to areas with fewer soundings. 25 points from prominent topographic features were added in the delta complex on the north side of the lake, and 20 additional interpolated points were added across the lake bottom to reduce artifacts in the bathymetric model. Geospatial data were integrated into a single bathymetric model in ArcMap using a tension spline with an output cell size of 2 m, a tension weight of 0.1, and 6 points-per-region.

3.5 Measured irradiance

PAR was measured under ice near solar noon at the 2014 dive site (Fig. 1) using a diver-deployed LI-1400 data logger with attached LI-192 cosine corrected underwater quantum detector (LI-COR Biosciences, Lincoln NE, USA). Divers swam transects immediately under the bottom of the ice cover and at approximately 1 m above the lake bottom following shore-parallel depth contours at 9, 12, and 15 m depths; they recorded PAR every 1-3 m. Percent surface irradiance was calculated from the average of pre- and post-dive surface values. Irradiance was also measured at the site of pH microelectrode deployments, but measurements are only available for the start of microelectrode deployment due to equipment failure.

3.6 Modeled irradiance

To compensate for the missing instrument data, 24-hour solar radiation exposure was modeled for the 2014 dive site (Fig. 1) over the duration of the pH microelectrode deployment. The ArcGIS solar radiation toolset was applied to this location and the 30 m DEM provided by LTER (www.mcmlter.org) to calculate incoming diffuse and direct solar radiation under default diffusivity parameterizations for a uniform and cloud-free sky. Elevation data was used to determine if direct radiation was blocked by local topography within the viewshed for a sun position calculated at a 10 minute interval (Fig. 3).

4 RESULTS

4.1 Environmental context and modern mat activity

4.1.1 Constraints on Lake Joyce bathymetry and lake level rise

Observations of recent lake level rise together with reconstructed bathymetry (Online Resource) extend previous records (Hawes et al., 2011) to provide a 68 year record of lake level. Shoreline contours from orthorectified aerial photographs are constrained at the meter-scale, with total RMS errors of less than 10 m for orthorectified ground control points. Aerial photographs (Fig. S2) indicate that shorelines in 1947 and 1961 were at average depth contours of 13 m and 11 m relative to 2014 lake level, respectively. Comparisons of 2010 and 2014 water column salinity profiles indicate that the shallow freshwater lens expanded by 1.4 m between 2010 and 2014. Together, these records demonstrate that lake level rose approximately 13 m over 68 years, for an average rise of 0.2 m yr^{-1} (see also Hawes et al., 2011).

Aerial photographs also indicate that properties of the Lake Joyce ice cover may have varied through time. In February 1947, the ice cover appears to have been broken into free floating fragments over a region 150 m by 350 m, with open water near inflowing streams and the moat extending >50 m from shore (Fig. S2). All other aerial photographs show an intact ice cover, which is more consistent with recent observations from field seasons in 2009, 2010, 2014, and 2015.

4.1.2 Water chemistry

Meltwater stream chemistry entering Lake Joyce from the Catspaw and Taylor glaciers (stream J5 from Green et al., 1988) varied significantly between the first and second sampling (a 24 hour difference). The first sampling had DIC concentrations of 0.11±0.01 mmol L^{-1} with $\delta^{13}C_{DIC}$ of -3.7±0.5‰ (1 SD, n=3) and $\delta^{18}O$ of -41.9±0.3‰. The second sampling had lower (but unmeasured) flow rates and the DIC concentrations were higher at 0.27±0.01 mmol L^{-1}, $\delta^{13}C_{DIC}$ was -0.3±0.1‰ (1 SD, n=3), and $\delta^{18}O$ was -41.4±0.3‰. The water column sample from 22 m depth had DIC concentrations of 2.0±0.2 mmol L^{-1} (1 SD, n=3), $\delta^{13}C_{DIC}$ was +2.8±0.3‰ (1 SD, n=3), and $\delta^{18}O$ was -41.4±0.06‰ (1 SD, n=3).

4.1.3 Measured PAR flux, modeled topographic shading and microelectrode pH profiles

PAR flux under the ice cover varied from 8 to 68 µmol photons m^{-2} s^{-1}, which was 0.6 to 5.4% of surface fluxes near solar noon. The mean transmission through the ice cover was 2.1±1.3% (1 SD, n=35). Irradiance decreased with depth in the lake, from 1.0±0.4% (1 SD, n=58) at 9 m to 0.7±0.4% (1 SD, n=33) at 12 m and 0.52±0.1% (1 SD, n=38) at 15 m (Table S2). PAR flux varied from high to low values over 10s of meters laterally at any given depth (Table S2). Modeled shading of the ice cover shows diurnal change in

sun exposure due to topographic shading on 23-24 November 2014 (Fig. 3). Modeled shading did not include the effect of clouds, which were present on 24 November 2014.

4.1.4 Mat pH

On the lake bottom, pH profiles through benthic microbial mats at 12 m varied spatially and through time. Near solar noon at 13:00-14:00, benthic PAR was 7.1 µmol photons m^{-2} s^{-1} and the ambient water column had a pH of 10.3. pH increased to 10.5 at the mat-water interface and exceeded 10.6 at 0.5-2 mm below the mat-water interface. pH fell below 10.5 at approximately 5 mm below the mat-water interface (Fig. 3). pH at the mat-water interface also varied through time on 23-24 November 2014, with maximum afternoon values of approximately 10.7 from 15:30 to 18:45, decreasing to 10.5 from 00:00 to 02:00 (Fig. 3).

4.2 Stromatolite petrography

Recurring patterns of induration and calcite textures allow division of the seven analyzed stromatolites into three calcified zones, separated by poorly lithified intervals containing disseminated blocky calcite (Fig. 4). The innermost zone 1 is heavily calcified (Fig. 4 C). Zone 2 consists of discontinuous layers and lenses of calcite with some poorly-calcified layers (Fig. 4 D). Zone 3 is the outermost and is composed of calcite crusts and botryoids in stromatolite branches (Fig. 4 E). Zone 3 is only present in stromatolites 2-7. Calcite zones 1, 2 and the first blocky layer of zone 3 in some stromatolites correspond to the morphological smooth growth zone of Mackey et al. (2015), whereas the remainder of calcite zone 3 correlates with the branched and irregular morphological growth zone.

The innermost interval, zone 1, averages 1.1±0.4 mm (1 SD, n=33) thick across the seven analyzed stromatolites. This zone consists of 1-2 layers of elongate to equant calcite up to 400 µm long that are isolated to intergrown. In the next layer toward the exterior of the stromatolites, similar intergrown blocky calcite served as the nucleation site for outward growing acicular calcite that forms botryoids and isopachous crusts (Fig. 4 C). The maximum thickness of this acicular calcite layer ranges from 400 to 1900 µm thick in different stromatolites, and the stromatolites with the thinnest acicular layer grew in the deepest water. The thicknesses of botryoids and isopachous crusts also systematically vary within individual

stromatolites; the thickest precipitates are near stromatolite peaks, and layers thin toward the bottom of the stromatolites. Crusts also thin where stromatolite surfaces were isolated from open water.

Zone 2 starts at the outer edge of the acicular layer with a 1.2±1.5 mm (1 SD, n=28) thick less heavily calcified interval. Within this interval, calcite is present as sparse isolated to intergrown 50 to 200 μm blocky calcite and discontinuous 100 to 1200 μm thick patches of microsparitic calcite with a fringe of blocky calcite. The next layers are typically 50 to 300 μm-thick and laterally discontinuous, but may also amalgamate to form ridges up to 3000 μm thick on the stromatolite side. Most layers are smooth at the mm-scale and are made up of intergrown blocky and microsparitic calcite. The outermost smooth layers of zone 2 also contain lenses of microsparitic calcite that are 200 to 1400 μm thick, extend more than 2000 μm vertically, and mimic the underlying layer morphology.

Zone 3 starts with a partially calcified layer that averages 3.0±1.5 mm (1 SD, n=19) thick and consists of disseminated 50 to 200 μm isolated to intergrown blocky equant to elongate calcite. This disseminated calcite layer is followed by intergrown blocky calcite that defines calcite layers, lenses or branches in stromatolites 2-7. Branches vary in length from mm- to cm-scale vertically, and the blocky calcite in branches averages 900 μm thick. In stromatolites 4-7, blocky calcite has outwardly projecting isopachous acicular calcite crusts and botryoids, which average 400 μm thick.

All calcified zones have 10 to 100 μm scale laminae bounded by horizons that contain more silt and clay sized siliciclastic sediment as well as microfossils consistent with cyanobacterial filaments. Stromatolites 1-3 and 5 were examined petrographically and have similar patterns in the thickness and organization of laminae within zone 1. Stromatolites 1-3 share patterns of sediment lamination in parts of the zone 1 acicular layer that allow lamina-by-lamina correlations. The patterns of laminae in the acicular layer of stromatolite 5 is similar to that of stromatolites 1-3, but the characteristics of individual laminae are not distinct enough for definitive correlation. Laminae within microsparitic and blocky calcite layers of calcified zones 2 and 3 are less consistent in number and thickness and have not been correlated. Both the predictable succession of calcite textures from the stromatolite interior to exterior and correlated laminae indicate that the stromatolites grew synchronously.

4.3 Stromatolite $\delta^{13}C$ and $\delta^{18}O$ records

4.3.1 $\delta^{13}C_{calcite}$

Stromatolites have $\delta^{13}C_{calcite}$ values that range from +3.9 to +9.6‰. $\delta^{13}C_{calcite}$ values vary from the inside to the outside of stromatolites, as well as within some individual layers on the sub-mm scale.

The innermost blocky calcite layer of zone 1 had $\delta^{13}C_{calcite}$ values of +7.4±0.3‰ (1 SD, n=8) in microdrilled stromatolites 1-3 (Fig. 5). Values for these stromatolites decrease to +5.7±0.5‰ (1 SD, n=9) in samples from the outer 500 µm normalized thickness of the zone 1 acicular calcite layer (Fig. 5). $\delta^{13}C_{calcite}$ values for the dissected layers of stromatolites 4 and 6 are consistent with the values from stromatolites 1-3, having a mean $\delta^{13}C_{calcite}$ value of +6.7±0.6‰ (1 SD, n=4) across the whole calcite zone 1. Stromatolites 5 and 7 generally have lower $\delta^{13}C_{calcite}$ values of +4.6±0.5‰ (1 SD, n=10) in zone 1 microdrilled and dissected calcite than stromatolites 1-4 and 6. $\delta^{13}C_{calcite}$ values in stromatolite 5 converge with those of stromatolites 1-4 and 6 by the end of zone 1.

In all stromatolites, $\delta^{13}C_{calcite}$ values increase from the inside to the outside of calcite zone 2 (Fig. 5). Overall, the mean $\delta^{13}C_{calcite}$ value of zone 2 in all stromatolites is +7.0±1.1‰ (1 SD, n=27), with the highest values present in the outer half of zone 2. Zone 3 is only present in stromatolites 2 and 5-7, and in these stromatolites $\delta^{13}C_{calcite}$ values increase from +6.9±1.3‰ (1 SD, n=18) in zone 2 to +8.2±0.3‰ (1 SD, n=16) in zone 3 (Fig. 5).

Overall, $\delta^{13}C_{calcite}$ values do not correlate with calcite texture, with acicular calcite present across the full range of $\delta^{13}C_{calcite}$ values of zone 1 as well as the highest $\delta^{13}C_{calcite}$ values of zone 3. Where measured in stromatolites 1 and 5 zone 1, samples across multiple locations in a single layer have smaller variations in $\delta^{13}C_{calcite}$ (0.3 to 1‰) than variations through the calcite zone, which exceed 2.4‰. Nevertheless, within these finely sampled stromatolites, $\delta^{13}C_{calcite}$ values do vary with the thickness of the acicular layer; $^{13}C/^{12}C$ ratios are higher where the acicular layer is thicker and lower where the acicular layer is thinner (Fig. S3).

4.3.2 $\delta^{18}O_{calcite}$

$\delta^{18}O_{calcite}$ values from all microdrilled and dissected stromatolites vary from -34.0‰ to -39.5‰ (Fig. 6). Within individual stromatolites, the lowest $\delta^{18}O_{calcite}$ values are in calcite zone 1, which has a mean $\delta^{18}O_{calcite}$ value of -37.7±1.0‰ (±1σ, n=41). Zones 2 and 3 have mean $\delta^{18}O_{calcite}$ values of -35.7±1.1‰ (±1 SD, n=26) and -36.3±0.7‰ (±1 SD, n=16), respectively. Values among different calcite zones overlap in

most stromatolites, but the mean value from zone 1 is significantly more depleted by >1‰ from that of zone 2 or zone 3 (t-test p-level <0.001). The variation between mean $\delta^{18}O_{calcite}$ values per zone within individual stromatolites is greatest in the shallowest stromatolite sampled, at 3.3‰. Variability in $\delta^{18}O_{calcite}$ values does not correlate to calcite texture.

4.3.3 $\delta^{13}C_{org}$

Surface microbial mat biomass was analyzed for $\delta^{13}C_{org}$ from stromatolite 8 at 22.1 m and a mat pinnacle at 16.6 m depth. At 22.1 m depth, $\delta^{13}C_{org}$ value was -22.1±0.3‰ (1 SD, n=3), whereas the $\delta^{13}C_{org}$ value at 16.6 m was -5.0±0.7‰ (1 SD, n=3). The 16.6 m samples had $\delta^{13}C_{org}$ values 14 to 18‰ lower than ambient $\delta^{13}C_{DIC}$ values measured for similar depths by Neumann et al. (2004). It is not possible to constrain fractionation between C_{org} and DIC for the stromatolite sample at 22.1 m depth due to poor constraints on $\delta^{13}C_{DIC}$ values at that depth, but the lower $\delta^{13}C_{org}$ values are consistent with generally decreasing $^{13}C/^{12}C$ ratios across the density gradient.

5 DISCUSSION

The Lake Joyce stromatolites grew in a changing environment, which can be reconstructed through a combination of historic lake level records, aerial photographs, stromatolite isotopic records, and measurements of the recent lake environment and photosynthetically active microbial mats. The combined data sets demonstrate that Lake Joyce stromatolites preserve records of microbial activity through decades of lake level rise.

5.1 Earliest stromatolite growth environments

5.1.1 Lake level and water column stratification

Aerial photographs of Lake Joyce from 1947 provide the earliest documentation of lake level and constrain the timing of the evolution of the density-stratified water column. Lake level rise observed since 1961 in Lake Joyce has primarily occurred through the expansion of the overriding freshwater lens (e.g. Gumbley, 1975; Hawes et al., 2011). Under this model for lake level rise, the bottom of the 2014 freshwater lens at 14.2 m depth would have been at 1.2 m in 1947, i.e. within the ice cover if it was a

similar thickness to that observed in 2014 (Mackey, 2016). Thus, the freshwater lens likely formed after 1947 as a product of mixing between meltwater influx and deeper, more saline water.

Prior to the establishment of the freshwater lens, saline water would have been in contact with the underside of the ice cover. During winter, freezing at the interface of the underside of the ice cover and the water column would have been necessary to replace ice lost from the surface via ablation (Dugan et al., 2013), and would have resulted in some penetrative convective mixing. Winter freezing of moat water could also have resulted in highly saline water, leading to intrusion of near-surface water into the density-stratified water column (c.f. Spigel and Priscu, 1998) and down-slope density currents (Miller and Aiken, 1996). In marginal areas of the lake, turbulent mixing between inflowing meltwater streams and the lake water in summer likely created water with variable salinities between the ice cover and the underlying lake water. Such mixing processes could have been extensive in years like 1947, when the ice cover fragmented and extensive meltwater moats developed.

5.1.2 Mixing waters and $\delta^{18}O_{calcite}$

In 1947, the lake bottom where columnar stromatolites grew would have been a few meters below the bottom of the ice cover at 8.8 to 10.0 m depth, close to the lake margin and within the steep density gradient (Fig. 7). Though there is no constraint on how long stromatolites were growing prior to 1947, this depth is consistent with Mackey et al.'s (2015) model for stromatolite initiation through buoyant liftoff of oxygen-rich gas bubbles in mat. Similar bubble liftoff mats forming from hyperoxic water columns have been reported to 11 m depth in nearby Lake Hoare (Wharton et al., 1983; Wharton et al., 1986) and 7.5 m depth in Lake Joyce (Mackey et al., 2015). The maximum depth of bubble liftoff is a product of hydrostatic pressure and dissolved gas concentration (e.g. Bosak et al., 2010), and thus interpretations of depth from the presence of bubble molds only provides a loose depth constraint contingent on dissolved gas concentration. Nevertheless, the significant increase in hydrostatic pressure with depth suggests that stromatolite initiation by bubble liftoff would only have been possible within a few meters of the underside of the ice cover. Thus, the earliest growth of Lake Joyce stromatolites likely took place within a few meters of the underside of the ice cover. This environment likely fluctuated significantly due to ice formation concentrating salts and seasonal meltwater influx. Thus, the stromatolites likely experienced significant changes in the water column with freshwater mixing and establishment of the freshwater lens after 1947.

This lake level history is consistent with changes in $\delta^{18}O_{calcite}$ values between stromatolite zone 1 and zone 2, which show an increase in $\delta^{18}O_{calcite}$ values (Fig. 8). This increase was likely caused by intrusions of relatively ^{18}O-enriched meltwater mixing (e.g. -33 to -34‰ from a regional alpine glacier source [Matsubaya et al., 1979]) mixing with long resident, ^{18}O-depleted freeze-concentrated saline lake water (e.g. -40 to -43‰ [www.mcmlter.org]) are consistent with the observed increase in $\delta^{18}O_{calcite}$ values between calcite zones 1 and 2. This mixing likely created or modified the pycnocline observed at 18.2 to 25.3 m depth in 2014. Given the ~4‰ difference in $\delta^{18}O_{H2O}$ across this pycnocline, evolution of the water column at the depth of stromatolites to more enriched $\delta^{18}O_{H2O}$ values would require relatively little mixing, and changing composition would likely dominate any potential signal from other factors, such as temperature (e.g. Kim and O'Neil, 1997; see supplemental materials). Indeed, the greatest increase in stromatolite $\delta^{18}O_{calcite}$ values was in the shallowest collected stromatolite, consistent in mixing of relatively enriched meltwaters into the depleted lake (Fig. 6). For a discussion of meltwater influx on $\delta^{13}C_{calcite}$, see supplemental materials.

5.1.3 Microbial effects on $\delta^{13}C_{calcite}$

Variable $\delta^{13}C_{calcite}$ values in stromatolites are most consistent with photosynthesis fractionating DIC within microbial mats and modifying $\delta^{13}C_{DIC}$ at the site of calcite precipitation. pH changes measured in microbial mats followed expected changes in irradiance from topographic shading, with decreasing pH during periods where microbial mats were shaded. Correlation of pH with irradiance suggests that microbial mat photosynthetic activity drove pH higher by uptake of HCO_3^- (e.g. Badger, 2003). See supplemental material for discussion of possible pH effects on $\delta^{13}C_{calcite}$ and $\delta^{18}O_{calcite}$. Because diffusion rates are slow enough to retain pH gradients in the Lake Joyce mats, a $\delta^{13}C_{DIC}$ gradient should be present as a result of preferential photosynthetic ^{12}C uptake (Sumner, 2001), and photosynthetic effects should be reflected by the $\delta^{13}C_{calcite}$ values of contemporaneous calcite.

The thickest parts of acicular layers had the most positive $\delta^{13}C_{calcite}$ values, suggesting that there is a positive correlation between the volume of calcite precipitation and the isotopic influence of photosynthesis. Thicker acicular layers could be a product of higher saturation indices due to locally higher pH associated with photosynthesis (e.g. Dupraz et al., 2009). Environmental variability early in stromatolite growth would have further affected the preservation of microbial effects on $\delta^{13}C_{calcite}$ values. The >5-fold

range of incident photon flux laterally under the Lake Joyce ice cover could account for the variation in zone 1 $\delta^{13}C_{calcite}$ values in different stromatolites, and the tendency for spatial variation in irradiance reaching the lake floor to be greatest in shallow, marginal regions (Hawes et al., 2011) may have contributed to this.

5.2 Stromatolite growth in a stratified water column

By the time Lake Joyce was again photographed in 1961, stromatolites were submerged to depths of 10.8 to 12.0 m. Thus, in 1961, the stromatolites were deeper than bubble disruption typically takes place (Wharton et al., 1983; Wharton et al., 1986). Bubble molds are present in the interior of calcite zone 1 (Mackey et al., 2015), suggesting that at least the initial layers of zone 1 lithified before 1961. Lake Joyce was also density stratified at the depths of stromatolite growth by 1961; the top of the primary pycnocline was at 7.2 m depth, significantly below the bottom of the ice cover. As stromatolites were growing at 10.8 to 12.0 m depths in 1961, they were likely within a consistent salinity gradient with little water mixing.

Water $^{18}O/^{16}O$ ratio was likely fixed by stratification under the freshwater lens before precipitation of calcite zone 2 and 3 with their more enriched calcite $^{18}O/^{16}O$ ratios (Fig. 6). The mean $\delta^{18}O_{calcite}$ values of calcite zones 2 and 3 are within 0.6‰ of each other, but the standard deviation of each zone is still 1.1‰ and 0.7‰, respectively. The variability in $\delta^{18}O_{calcite}$ values under consistent $\delta^{18}O_{H2O}$ values requires a change in the fractionation between H_2O and calcite. Temperature variations leading to a change in the fractionation between H_2O and calcite (e.g. Kim and O'Niel, 1997) were likely minimal in Lake Joyce, given the small observed changes in temperature year-to-year and moderation of temperature by perennial contact with the ice cover and Taylor Glacier (Spigel and Priscu, 1998). Variation in fractionation could instead be due to pH variation (e.g. Spero et al., 1997; Zeebe, 1999) or kinetic effects from seasonal changes in calcite saturation state (Dietzel et al., 2009; see supplemental materials for further discussion).

5.2.1 Evolution of DIC $^{13}C/^{12}C$ ratios in an isolated water body

By the time that calcite zone 2 precipitated, the primary exchange of DIC across density gradients would have been through chemical diffusion (e.g. Spigel and Priscu, 1998). Accordingly, stromatolite calcite precipitated out of an isolated DIC reservoir, and any changes in the $\delta^{13}C_{calcite}$ reflect local processes modifying the DIC $^{13}C/^{12}C$ ratios in the microbial mat calcifying environment or the ambient DIC pool

(Wharton et al., 1993). With increasing lake level, variability in photosynthetic fractionation effects on the local DIC $^{13}C/^{12}C$ ratio likely decreased on the stromatolite growth surface. Photosynthetic rates would become more uniform among stromatolites as variability in incident irradiance decreased with increasing depth (e.g. Hawes et al., 2011). Changes in $\delta^{13}C_{calcite}$ through zone 2 and into zone 3 are most consistent with long-term preferential photosynthetic ^{12}C removal from the ambient DIC pool, rather than local microbial effects. If enrichment were due to local microbial activity, the increase in $\delta^{13}C_{calcite}$ would require an increasing photosynthetic signature through time, which is contradicted by the predicted reduction in illumination, and thus photosynthetic rates, with lake level rise (Hawes et al., 2011; for discussion of fractionation factors, see supplemental materials).

5.3 Cessation of stromatolite photosynthetic growth

Before 2009, lake level rise had reduced irradiance to levels below that necessary for net photosynthetic growth (Hawes et al., 2011). The maximum depth for net photosynthetic growth was at 13 and 16 m in 2009 and 2010, respectively (Hawes et al., 2011; Fig. 7). The end of growth is thus bracketed by 1991, when stromatolites were first submerged below 16 m, and 2009 when direct observations demonstrated that stromatolites were no longer growing (Hawes et al., 2011). Evidence of this transition to net heterotrophy is lacking from the outermost calcite precipitates in zone 3, which suggests that heterotrophic activity is low (e.g. Hawes and Schwarz, 1999) or a lack of calcite precipitation during stromatolite decomposition.

5.5 Application to paleolake deposits

Results from Lake Joyce can provide insights into the record of environmental change preserved in deposits from ice-covered paleolakes. Paleolake deposits, including radiocarbon-dated relic microbial mats, have been used to assess the age and extent of larger lakes that occupied the McMurdo Dry Valleys during previous glacial maxima (Clayton-Greene et al., 1988; Doran et al., 1998; Hall et al., 2002; see Berger et al., 2013 for discussion of radiocarbon versus photon stimulated luminescence in these deposits). As one example, paleolake deposits from the last glacial maximum in Victoria Valley, McMurdo Dry Valleys, contain abundant sand mounds, which are characteristic deposits of ice-covered lakes (Squyres et

al., 1991). The Victoria Valley sand mounds also contain relic benthic microbial mats with associated calcite (Doran et al., 1998; Hall et al., 2002), making them ideal comparisons for the Lake Joyce deposits. The $\delta^{13}C_{calcite}$ values in this area span +2.30‰ to +3.95‰, and most associated microbial mat $\delta^{13}C_{org}$ values are significantly depleted relative to calcite (Hall et al., 2002). The range of $\delta^{13}C_{calcite}$ values is much smaller than found in zone 1 of Lake Joyce stromatolites, but is similar to the range in the outer part of zone 2 into zone 3. Applying the relationships interpreted from $\delta^{13}C_{calcite}$ values of Lake Joyce stromatolites, the low variability in sand mound carbonates could be due to a lower photosynthetic rate relative to DIC concentration with little lateral variability in illumination. Lower photosynthetic rates would be consistent with observed fractionation between mats and calcite, similar to deeper photosynthetic communities found in modern MDV lakes (Lawson et al., 2004). The $\delta^{13}C_{calcite}$ values are also lower than typically found in Lake Joyce, and may represent little photosynthetic modification of the ambient carbon pool, or lower initial $\delta^{13}C_{DIC}$ values. Such hypotheses could be tested by more detailed stratigraphic exploration of the carbonates, investigating whether trends within individual carbonate layers have sub-mm scale heterogeneity in $\delta^{13}C_{calcite}$ values consistent with photosynthetic modification of an ambient DIC pool.

The interpretation of isotopic signatures in paleolake deposits requires the integration of paleohydrologic data, as shown in this study. Stromatolites in Lake Joyce provide carbon isotopic records with non-unique solutions. Without independent evidence of lake level rise associated with Lake Joyce stromatolite growth, the record of gradual increase in $\delta^{13}C_{calcite}$ values presented here could be interpreted as a product of increasing photosynthetic rates during falling lake levels. Rather, the integration of hydrologic records suggests the signatures result from the long-term water column stratification and heterogeneous light environments of a perennially ice-covered lake. Thus, it is necessary to augment general observations of $\delta^{13}C_{calcite}$ value variability with other evidence of stratification or changing water sources such as $\delta^{18}O_{calcite}$ values. Future work exploring evidence of changes in salinity through calcite major and trace element chemistry (e.g. Okumura and Kitano, 1986) could help deconvolve the complex isotopic record of carbonates. The case study of Lake Joyce stromatolites demonstrates that detailed analysis of paleolake deposits could shed new light on variability in lake environments associated with changing climate in the McMurdo Dry Valleys.

6 CONCLUSIONS

Calcitic stromatolites in Lake Joyce mineralized during a period of lake level rise, providing a test for the use of calcite $\delta^{18}O$ and $\delta^{13}C$ values to reconstruct co-occurring changes in lake conditions and microbial activity. Trends in isotopic ratios of Lake Joyce stromatolites record evidence of variable source waters and photosynthetic rates during stromatolite growth. The earliest stromatolite layers (calcite zone 1) have $\delta^{13}C_{calcite}$ values that vary both within individual stromatolites and among stromatolites. Variability in $\delta^{13}C_{calcite}$ values is consistent with a large range of photosynthetic rates in a heterogeneous irradiance environment close to the underside of the ice cover. Zone 1 $\delta^{18}O_{calcite}$ values are also lower than subsequent zones, which is most consistent with mixing in between of inflowing meltwater and saline lake water immediately under the ice cover. Subsequent precipitation of calcite zones 2 and 3 took place as lake levels rose. Rising lake levels led to lower and more uniform irradiance and created a density stratified lake structure that isolated the ambient water from mixing. Lower, more consistent PAR fluxes reduced local photosynthetic effects on $\delta^{13}C_{calcite}$ values, and the isolated ambient DIC pool evolved to higher $\delta^{13}C_{DIC}$ values over decades of net photosynthesis.

Stromatolite $\delta^{13}C_{calcite}$ values support hypotheses for environmental reconstructions based on benthic carbonates of perennially ice-covered lakes: 1) $\delta^{13}C_{calcite}$ values are most variable under conditions with heterogeneous water chemistry, particularly in shallow regions of lakes with lateral variability in irradiance and photosynthetic activity, and 2) $\delta^{13}C_{calcite}$ values are less variable where photosynthesis is not sufficiently rapid to change local $\delta^{13}C_{DIC}$ with preferential uptake of ^{12}C. Such conditions are most consistent with the lower irradiance limit for photosynthesis in MDV lakes. Trends in isotopic values can constrain primary productivity in polar meltwater oases, particularly where other sedimentological evidence indicates the presence of a perennial ice cover. Interpretation of environmental change from general trends in $\delta^{13}C_{calcite}$ values require analyses at the scale of heterogeneous microbial activity and supporting evidence for the nature of lake stratification or mixing like $\delta^{18}O_{calcite}$. Without detailed investigation of $\delta^{13}C_{calcite}$ value heterogeneity and evidence for stratification from $\delta^{18}O_{calcite}$, the general increase in $\delta^{13}C_{calcite}$ values through stromatolite growth could have been interpreted as evidence for higher rates of photosynthesis and lake level fall rather than chemical isolation by stratification in the course of lake level rise.

REFERENCES

Andersen DT (2007) Antarctic inland waters: scientific diving in the perennially ice-covered lakes of the McMurdo Dry Valleys and Bunger Hills. In: International Polar Diving Workshop (eds Lang MA, Sayer MDJ). Smithsonian Institution, Washington, DC, Svalbard, pp. 213.

Andersen DW, Wharton RA, Squyres SW (1993) Terrigenous clastic sedimentation in Antarctic dry valley lakes. In: Physical and Biogeochemical Processes in Antarctic Lakes (eds Green WJ, Friedman EI). American Geophysical Union, Washington, DC.

Andres MS, Sumner DY, Reid RP, Swart PK (2006) Isotopic fingerprints of microbial respiration in aragonite from Bahamian stromatolites. Geology, 34, 973-976. doi: 10.1016/j.sedgeo.2005.12.020

Badger MR, Price GD (2003) CO_2 concentrating mechanisms in cyanobacteria: molecular components, their diversity and evolution. Journal of Experimental Botany, 54, 609-622. doi.org/10.1093/jxb/erg076

Berger GW, Doran PT, Thomsen KJ (2013) Micro-hole and multigrain quartz luminescence dating of Paleodeltas at Lake Fryxell, McMurdo Dry Valleys (Antarctica), and relevance for lake history. Quaternary Geochronology, 18, 119-134. doi: 10.1016/j.quageo.2013.04.002

Bosak T, Bush JW, Flynn MR, Liang B, Ono S, Petroff AP, Sim MS. (2010) Formation and stability of oxygen- rich bubbles that shape photosynthetic mats. Geobiology, 8, 45-55. doi:10.1111/j.1472-4669.2009.00227.x

Brady AL, Druschel G, Leoni L, Lim DSS, Slater G (2013) Isotopic biosignatures in carbonate-rich, cyanobacteria-dominated microbial mats of the Cariboo Plateau, B.C. Geobiology, 11, 437-456. doi: 10.1111/gbi.12050

Bockheim JG, McLeod M (2013) Glacial geomorphology of the Victoria Valley System, Ross Sea Region, Antarctica. Geomorphology, 193, 14-24. doi: 10.1016/j.geomorph.2013.03.020

Castendyk DN, Obryk MK, Leidman SZ, Gooseff M, Hawes I (2016) Lake Vanda: A sentinel for climate change in the McMurdo Sound Region of Antarctica. Global and Planetary Change, 144, 213-227. doi: 10.1016/j.gloplacha.2016.06.007

Chinn TJ (1993) Physical Hydrology of the Dry Valley Lakes. In: Physical and Biogeochemical Processes in Antarctic Lakes (eds Green WJ, Friedman EI). American Geophysical Union, Washington, DC.

Clayton-Greene JM, Hendy CH, Hogg AG (1988) Chronology of a Wisconsin age proglacial lake in Miers Valley, Antarctica. New Zealand Journal of Geology and Geophysics, 31, 353-361. doi: 10.1080/00288306.1988.10417781

Convey P, Chown SL, Clarke A, Barnes DKA, Bokhorst S, Cummings V, Ducklow HW, Frati F, Green TGA, Gordon S, Griffiths HJ, Howard-Williams C, Huiskes AHL, Laybourn-Parry J, Lyons WB, McMinn A, Morley SA, Peck LP, Quesada A, Robinson SA, Schiaparelli S, Wall DH (2014) The spatial structure of Antarctic biodiversity. Ecological Monographs, 84, 203-244. doi: 10.1890/12-2216.1

Dietzel M, Tang J, Leis A, Köhler SJ (2009) Oxygen isotopic fractionation during inorganic calcite precipitation – Effect of temperature, precipitation rate and pH. Chemical Geology, 268, 107-115. doi: 10.1890/12-2216.1

Doran PT, Wharton RAJ, Lyons WB (1994) Paleolimnology of the McMurdo Dry Valleys, Antarctica. Journal of Paleolimnology, 10, 85-114. doi:10.1007/BF00682507

Doran PT, Wharton RAJ, Des Marais DJ, McKay CP (1998) Antarctic paleolake sediments and the search for extinct life on Mars. Journal of Geophysical Research, 103, 28481-28493. doi: 10.1029/98JE01713

Doran PT, McKay CP, Clow GD, Dana GL, Fountain AG, Nylen T, Lyons WB (2002) Valley floor climate observations from the McMurdo dry valleys, Antarctica, 1986-2000. Journal of Geophysical Research, 107, 4772. doi:10.1029/2001JD002045

Doran PT, McKay CP, Fountain AG, Nylen T, McKnight DM, Jaros C, Barrett JE (2008) Hydrologica response to extreme warm and cold summers in the McMurdo Dry Valleys, East Antarctica. Antarctic Sciences, 20, 499-509. doi:10.1017/S0954102008001272

Dugan HA, Obryk MK, Doran PT (2013) Lake ice ablation rates from permanently ice-covered Antarctic lakes. Journal of Glaciology, 59, 491-498. doi:10.3189/2013JoG12J080

Dupraz CR, Reid RP, Braissant P, Decho AW, Norman RS, Visscher PT (2009) Processes of carbonate precipitation in modern microbial mats. Earth-Science Reviews, 96, 141-162. doi: 10.1007/BF00682507

Fountain AG, Lyons WB, Burkins, Dana GL, Doran PT, Lewis KJ, McKnight DM, Moorhead DL, Parsons AN, PRiscu JC, Wall DH, Wharton RA, Virginia RA (1999) Physical controls on the Taylor Valley ecosystem, Antarctica. BioScience, 49, 961-971. doi.org/10.1525/bisi.1999.49.12.961

Gooseff MN, McKnight DM, Doran P, Fountain AG, Lyons WB (2011) Hydrological connectivity of the landscape of the McMurdo Dry Valleys, Antarctica. Geography Compass, 5, 666-681. doi: 10.1111/j.1749-8198.2011.00445.x

Green WJ, Angle MP, Chave KE (1988) The geochemistry of Antarctic streams and their role in the evolution of four lakes of the McMurdo Dry Valleys. Geochimica Et Cosmochimica Acta, 52, 1265-1274. doi: 10.1016/0016-7037(88)90280-3

Green WJ, Lyons WB (2009) The saline lakes of the McMurdo Dry Valleys, Antarctica. Aquatic Geochemistry, 15, 321-348. doi: 10.1007/s10498-008-9052-1

Gumbley JW (1975) A sedimentological study of three saline lakes in the Dry Valleys of Victoria Land, Antarctica. In: Earth Science Department. University of Waikato.

Hall BL, Denton GH, Overturf B, Hendy CH (2002) Glacial Lake Victoria, a high-level Antarctic lake inferred from lacustrine deposits in Victoria Valley. Journal of Quaternary Science, 17, 697-706. doi: 10.1002/jqs.691

Hall CM, Castro MC, Kenig F, Doran PT (2017) Constraining the recent history of the perennially ice-covered Lake Bonney, East Antarctica using He, Kr and Xe concentrations. Geochimica et Cosmochimica Acta, 209, 233-253. doi: 10.1016/j.gca.2017.04.023

Hawes I, Jungblut AD, Obryk M, Doran P (2016) Growth dynamics of a laminated microbial mat in response to variable irradiance in an Antarctic lake. Freshwater Biology, 61, 396-410. doi: 10.1111/fwb.12715

Hawes I, Schwarz A-M (1999) Photosynthesis in an extreme shade environment: benthic microbial mats from Lake Hoare, a permanently ice-covered Antarctic Lake. Journal of Phycology, 35, 448-459. doi: 10.1046/j.1529-8817.1999.3530448.x

Hawes I, Sumner DY, Andersen DT, Mackey TJ (2011) Legacies of recent environmental change in the benthic communities of Lake Joyce, a perennially ice-covered Antarctic lake. Geobiology, 9, 394-410. doi: 10.1111/j.1472-4669.2011.00289.x

Hawes, I., Giles, H. and Doran, P. T. 2014. Estimating photosynthetic activity in microbial mats in an ice-covered Antarctic lake using automated oxygen microelectrode profiling and variable chlorophyll fluorescence. *Limnology and Oceanography*. 59: 674-688

Hendy CH, Hogg AG, Hosking PL, Oliver TI (1973) Antarctic Research Unit Report no. 3. University of Waikato, pp. 6.

Hendy CH, Healy TR, Rayner EM, Shaw J, Wilson AT (1979) Late Pleistocene glacial chronology of the Taylor Valley, Antarctica, and the global climate. Quaternary Research, 11, 172-184.

Hendy CH, Sadler AJ, Denton GH, Hall BL (2000) Proglacial lake-ice conveyors: A new mechanism for deposition of drift in polar environments. Geografiska Annaler, 82, 249-270. doi: 10.1111/j.0435-3676.2000.00124.x

Hendy CH, Hall BL (2006) The radiocarbon reservoir effect in proglacial lakes: Examples from Antarctica. Earth and Planetary Science Letters, 241, 413-421. doi: 10.1016/j.epsl.2005.11.045

Howard-Williams C, Schwarz A-M, Hawes I, Priscu JC (1998) Optical Properties of the McMurdo Dry Valleys Lakes, Antarctica. In: Ecosystem Dynamics in a Polar Desert: the McMurdo Dry Valleys (ed Priscu JC). American Geophysical Union, pp. 189-202.

Kim ST, O'Neil JR (1997) Equilibrium and nonequilibrium oxygen isotope effects in synthetic carbonates. Geochimica et Cosmochimica Acta, 61, 3461-3475.

Knoepfle JL, Doran PT, Kenig F, Lyons WB, Galchenko VF (2009) Particulate organic and dissolved inorganic carbon stable isotopic compositions in Taylor Valley lakes, Antarctica: the effect of legacy. Hydrobiologia, 632, 139-156. doi: 10.1007/s10750-009-9834-5

Kreylos O (2008) Environment-Independent VR Development. In: Advances in Visual Computing Bebis G. et al. (eds). ISVC 2008. Lecture Notes in Computer Science, vol 5358. Springer, Berlin, Heidelberg.

Lawrence MJF, Hendy CH (1985) Water column and sediment characteristics of Lake Fryxell, Taylor Valley, Antarctica. New Zealand Journal of Geology and Geophysics, 28, 543-552. doi: 10.1080/00288306.1985.10421206

Lawson J, Doran PT, Kenig F, Des Marais DJ, Priscu JC (2004) Stable carbon and nitrogen isotopic composition of benthic and pelagic organic matter in lakes of McMurdo Dry Valleys, Antarctica. Aquatic Geochemistry, 10, 269-301. doi: 10.1007/s10498-004-2262-2

Lyons WB, Tyler SW, Wharton RA, McKnight DM, Vaughn BH (1998) A Late Holocene desiccation of Lake Joare and Lake Fryxell, McMurdo Dry Valleys, Antarctica. Antarctic Science, 10, 247-256. doi: 10.1017/S0954102098000340

Mackey TJ, Sumner DY, Hawes I, Jungblut AD, Andersen DT (2015) Growth of modern branched columnar stromatolites in Lake Joyce, Antarctica. Geobiology, 13, 373-390. doi: 10.1111/gbi.12138

Mackey TJ, Sumner DY, Hawes I, Jungblut AD, Lawrence J, Leidman S, Allen B (2017) Increased mud deposition reduces stromatolite complexity. Geology, 45, 663-666. doi: 10.1130/G38890.1

Matsubaya O, Sakai H, Torii T, Burton H, Kerry K (1979) Antarctic saline lakes -- stable isotopic ratios, chemical compositions and evolution. Geochimica et Cosmochimica Acta, 43, 7-25. doi: 10.1016/0016-7037(79)90042-5

McKay CP, Clow CD, Andersen DT, Wharton RAJ (1994) Light transmission and reflection in perennially ice-covered Lake Hoare, Antarctica. Journal of Geophysical Research, 99, 20427-20444. doi: 10.1029/94JC01414

Miller LG, Aiken GR (1996) Effects of Glacial Meltwater Inflows and Moat Freezing on Mixing in an Ice-Covered Antarctic Lake as Interpreted from Stable Isotope and Tritium Distributions. Limnology and Oceanography, 41, 966-976. doi: 10.4319/lo.1996.41.5.0966

Moorhead D, Schmeling J, Hawes I (2005) Modelling the contribution of benthic microbial mats to net primary production in Lake Hoare, McMurdo Dry Valleys. Antarctic Science, 17, 33-45. doi: 10.1017/S0954102005002403

Neumann K, Lyons WB, Priscu JC, DesMarais DJ, Welch KA (2004) The carbon isotopic composition of dissolved inorganic carbon in perennially ice-covered Antarctic lakes: searching for a biogenic signature. Annals of Glaciology, 39, 518-524. doi: 10.3189/172756404781814465

Okumura M, Kitano Y (1986) Coprecimiptation of alkali metal ions with calcium carbonate. Geochiica et Cosmochimica Acta, 50, 49-58.

O'Neil JR (1968) Hydrogen and Oxygen Isotope Fractionation between Ice and Water. Journal of Physical Chemistry, 72, 3683-3684.

Quesada A, Fernández-Valiente E, Hawes I, Howard-Williams C (2008) Benthic primary production in polar lakes and rivers. In: Polar Lakes and Rivers (eds Vincent WF, Laybourn-Parry J). Oxford Scholarship Online Monographs, pp. 179-194.

Schenk T, Csathó B, Ahn Y, Yoon T, Shin SW, Huh KI (2004) DEM generation from the Antarctic LiDAR data: Site report. US Geological Survey.

Shacat JA, Green WJ, DeCarlo EH, Newell S (2004) The Geochemistry of Lake Joyce, McMurdo Dry Valleys, Antarctica. Aquatic Geochemistry, 10, 325-352. doi: 10.1023/B:AQUA.0000047184.50027.41

Spero HJ, Bijma J, Lea DW, Bemis BE (1997) Effect of seawater carbonate concentration on foraminiferal carbon and oxygen isotopes. Nature, 390, 497-500. doi: 10.1038/37333

Spigel RH, Priscu JC (1998) Physical Limnology of the McMurdo Dry Valleys Lakes. In: Ecosystem Dynamics in a Polar Desert: the McMurdo Dry Valleys, Antarctica (ed Priscu JC). American Geophysical Union, Washington, DC.

Squyres SW, Andersen DW, Nedell SS, Wharton RA (1991) Lake Hoare, Antarctica: sedimentation through a thick perennial ice cover. Sedimentology, 38, 363-379. doi: 10.1111/j.1365-3091.1991.tb01265.x

Stevens EW, Sumner DY, Harwood CL, Crutchfield J, Hamann B, Kreylos O, Puckett E, Senge P (2011) Understanding Microbialite Morphology Using a Comprehensive Suite of Three-Dimensional Analysis Tools. Astrobiology, 11, 509-518. doi: 10.1089/ast.2010.0560

Sumner DY (2001) Microbial Influences on Local Carbon Isotopic Ratios and Their Preservation in Carbonate. Astrobiology, 1, 57-70. doi: 10.1089/153110701750137431

Sutherland DL, Hawes I (2009) Annual growth layers as proxies of past growth conditions for benthic microbial mats in a perennially ice-covered Antarctic lake. FEMS Microbiological Ecology, 67, 279-292. doi:10.1111/j.1574-6941.2008.00621.x

Suzuoki T, Kimura T (1973) D/H and 18O/16O Fractionation in Ice-Water system. Mass Spectroscopy, 21, 229-233. doi: 10.5702/massspec1953.21.229

Wharton RA, McKay CP, Simmons GMJ, Parker BC (1986) Oxygen Budget of a Perennially Ice-Covered Antarctic Lake. Limnology and Oceanography, 31, 437-443. doi: 10.4319/lo.1986.31.2.0437

Wharton RA, Parker BC, Simmons GM, Seaburg KG, Love FG (1982) Biogenic calcite structures forming in Lake Fryxell, Antarctica. Nature, 295, 403-405.

Wharton RAJ, Parker BC, Simmons GMJ (1983) Distribution, species composition and morphology of algal mats in Antarctic dry valley lakes. Phycologia, 22, 355-365. doi: 10.2216/i0031-8884-22-4-355.1

Wilson AT (1964) Evidence from chemical diffusion of a climatic change in the McMurdo dry valleys 1200 years ago. Nature, 201, 176-177. doi: 10.1038/201176b0

Zeebe RE (1999) An explanation of the effect of seawater carbonate concentration on foraminiferal oxygen isotopes. Geochimica et Cosmochimica Acta, 63, 2001-2007. doi: 10.1016/S0016-7037(99)00091-5

Zhang L, Jungblut AD, Hawes I, Andersen DT, Sumner DY, Mackey TJ (2015) Cyanobacterial diversity in benthic mats of the McMurdo Dry Valley lakes, Antarctica. Polar Biology, 38, 1097-1110. doi: 10.1007/s00300-015-1669-0

FIGURE CAPTIONS AND DATA TABLE

Figure 1: The McMurdo Dry Valleys, Antarctica (A) contain perennially ice-covered lakes like Lake Joyce (B). Lake Joyce abuts Taylor Glacier and is fed by seasonal meltwater streams (C; terminology after Green et al., 1988). Lake outline from 2010 (B) shows the location of water column sample site and the dive holes (DH) used for collecting stromatolites and mat samples.

Figure 2: Cluster of branched columnar stromatolites from 23 m depth in Lake Joyce. Squares on float are 1 cm^2.

Figure 3: Microelectrode surveys of microbial mat at 12.1 m depth and modeled irradiance. A) pH within the microbial mat diffusive boundary layer across a diurnal cycle 23-24 November 2014. Modeled irradiance for a diurnal cycle at the sampling site in Lake Joyce superimposed on the pH profile. Actual irradiance on 24 November 2014 was more variable than modeled due to clouds. B) Two microelectrode profiles (white versus black points) through microbial mat near solar noon on 23 November 2014.

Figure 4: Details of sampled stromatolite 2 from 22.1 m depth. A) Upright stromatolite sampled in growth orientation within push core, including underlying sand. B) Freeze-dried slice cut from stromatolite with calcite zone separated by dashed lines and boxes marking approximate locations of C-D: C) thin section photomicrograph of blocky and acicular calcite from calcite zone 1, D) layers within calcite zone 2, and E) blocky calcite within calcite zone 3.

Figure 5: $\delta^{13}C_{calcite}$ values for each stromatolite placed on a shared axis of normalized stromatolite radius (black) in comparison to all stromatolite $\delta^{13}C_{calcite}$ values (grey). Bold samples were microdrilled, and the length of the bold lines indicates the proportion of the calcite zone that was sampled with the microdrill raster. Dashed lines denote samples from dissected stromatolites. In zone 1 and 3, line length indicates the fraction of the zone homogenized for the sample, whereas in zone 2, smaller subsamples of individual layers were homogenized and the line length indicates the extent to which sample sites could be correlated to the normalized stromatolite radius.

Figure 6: Mean stromatolite $\delta^{18}O_{calcite}$ values for each calcite zone. Error bars on each stromatolite are 1 standard deviation where 3 or more samples were collected for the stromatolite zone. The grey box in each zone marks the mean ± 1 standard deviation of $\delta^{18}O_{calcite}$ values for all stromatolites in that zone.

Figure 7: Interpreted environmental context for stromatolite growth based on lake levels in A) 1947 and B) 1961 aerial photographs and C) lake level measured in 1991. Conductivity profile in all panels from 2014, with hypothized mixing between deep saline waters to generate the observed pycnocline (A) followed by lake level rise accommodated by thickening of the freshwater lens (B). Under low lake levels bubble liftoff

could lead to stromatolite initiation (A). Lake level rise by 1961 would have reduced bubble growth and liftoff of the benthic mat, and density stratification would have led to isolation of the ambient water (B). By 1991, stromatolites would have been at a depth with insufficient irradiance for net photosynthetic growth (C).

Figure 8: Summary of $\delta^{13}C$ versus $\delta^{18}O$ for stromatolites and their surrounding environment. All $\delta^{13}C_{DIC}$ and $\delta^{18}O_{H2O}$ have been recalculated as equilibrium values for calcite precipitated in 0 °C water for direct comparison with stromatolite calcite. General trends in stromatolite $\delta^{13}C$ and $\delta^{18}O$ values are marked with arrows for stromatolites 1-4 and 6 (solid) and stromatolites 5 and 7 (dashed). All stromatolites generally trend toward higher $\delta^{18}O$ values in the course of growth as $\delta^{13}C$ become more uniform. $\delta^{18}O$ values for alpine and Taylor glaciers span the range of mean values reported in Matsubaya et al. (1979), Stuiver et al. (1981), and Gooseff et al. (2006, Taylor Glacier only); alpine glacier values are taken from the Rhone Glacier near Lake Joyce. $\delta^{13}C$ values for glaciers come from meltwater stream values throughout the McMurdo Dry Valleys region. The light grey range spans typical values, whereas the dark grey range spans the flow-weighted mean values entering Taylor Valley lakes (Neumann, 1999; Lyons et al., 2013).

Calcite $\delta^{13}C$ and $\delta^{18}O$ analyses			
Sample	Depth (m)	Site	Processing
Stromatolite 1	21.8	2010 DH	Microdrilled
Stromatolite 2	22.1	2010 DH	Microdrilled
Stromatolite 3	22.4	2010 DH	Microdrilled
Stromatolite 4	22.4	2010 DH	Dissected
Stromatolite 5	22.4	2009 DH	Microdrilled/Dissected
Stromatolite 6	23.0	2009 DH	Dissected
Stromatolite 7	--	~80 m SE of 2009 DH	Microdrilled/Dissected

Organic $\delta^{13}C$ analyses			
Sample	Depth (m)	Site	Processing
Stromatolite 8	22.1	2010 DH	Dissected
Bulbous pinnacle	16.6	2010 DH	Dissected

Table 1: Stromatolites sampled in Lake Joyce. Depth constraints are ±0.3 m from dive computers

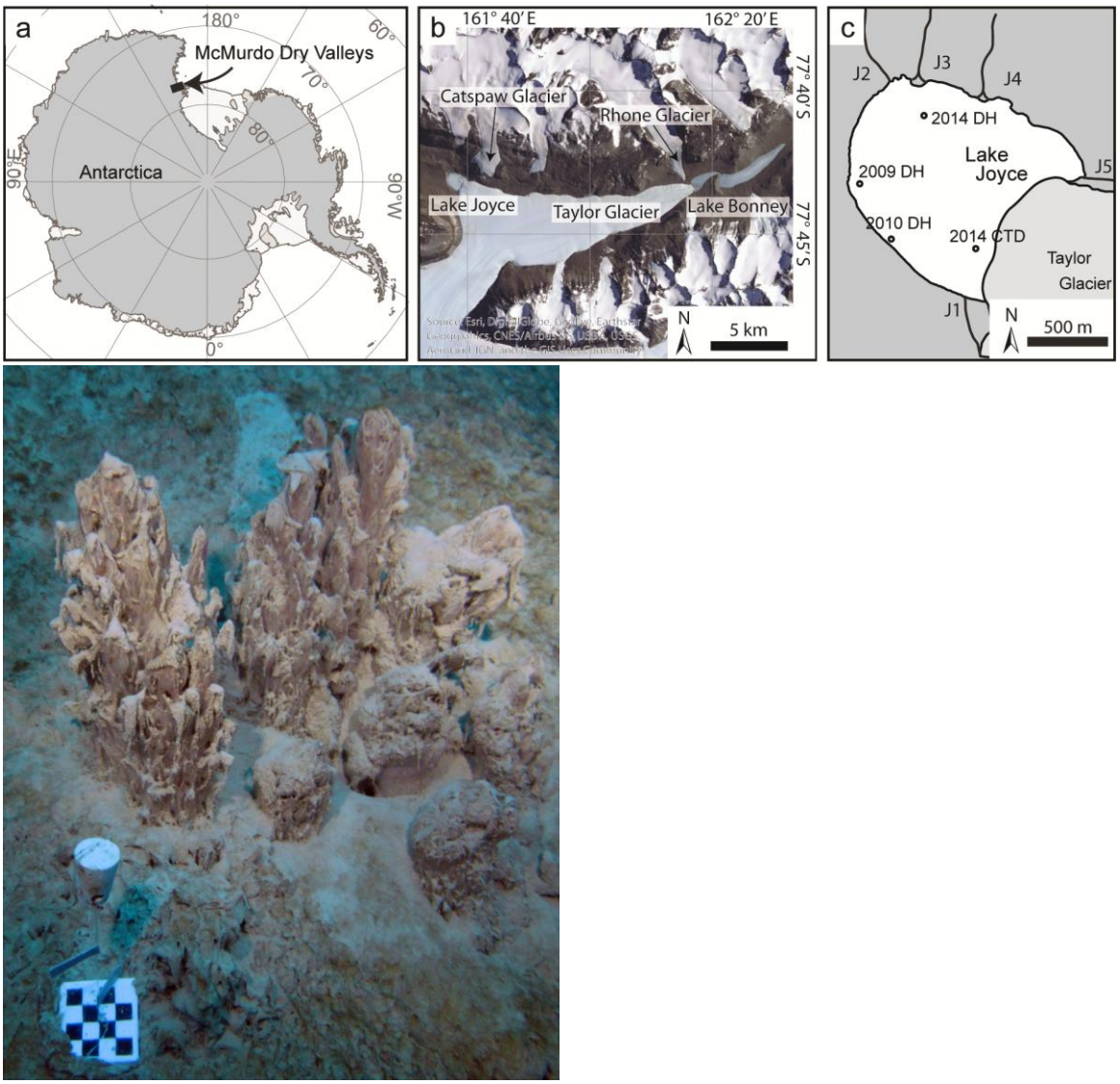
a
180°
60°
70°
80°
90°E
90°W
0°
McMurdo Dry Valleys
Antarctica
b
161° 40′ E
162° 20′ E
77° 40′ S
77° 45′ S
Catspaw Glacier
Rhone Glacier
Lake Joyce
Taylor Glacier
Lake Bonney
N
5 km
c
J2
J3
J4
J5
J1
2014 DH
2009 DH
2010 DH
2014 CTD
Lake
Joyce
Taylor
Glacier
N
500 m

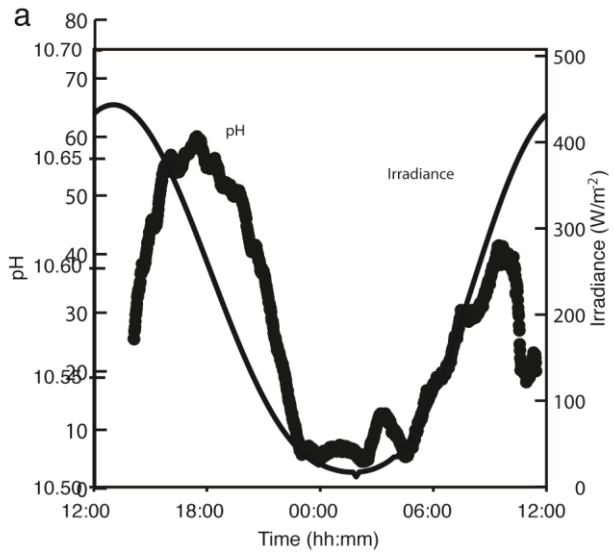
a
pH
Irradiance
Irradiance (W/m-2)
Time (hh:mm)
12:00
18:00
00:00
06:00
12:00

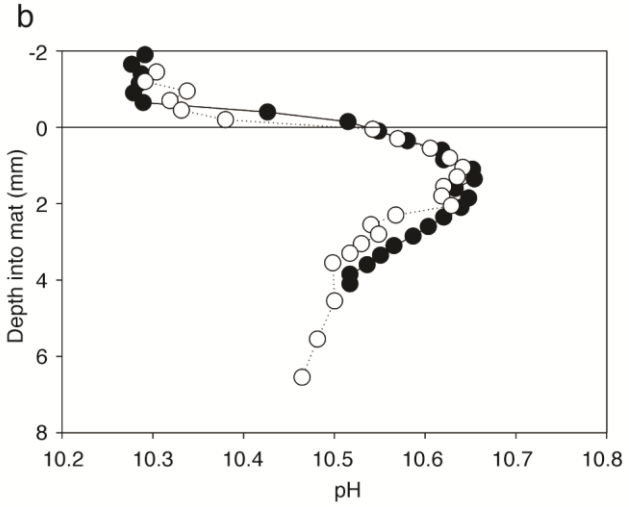
b
Depth into mat (mm)
pH

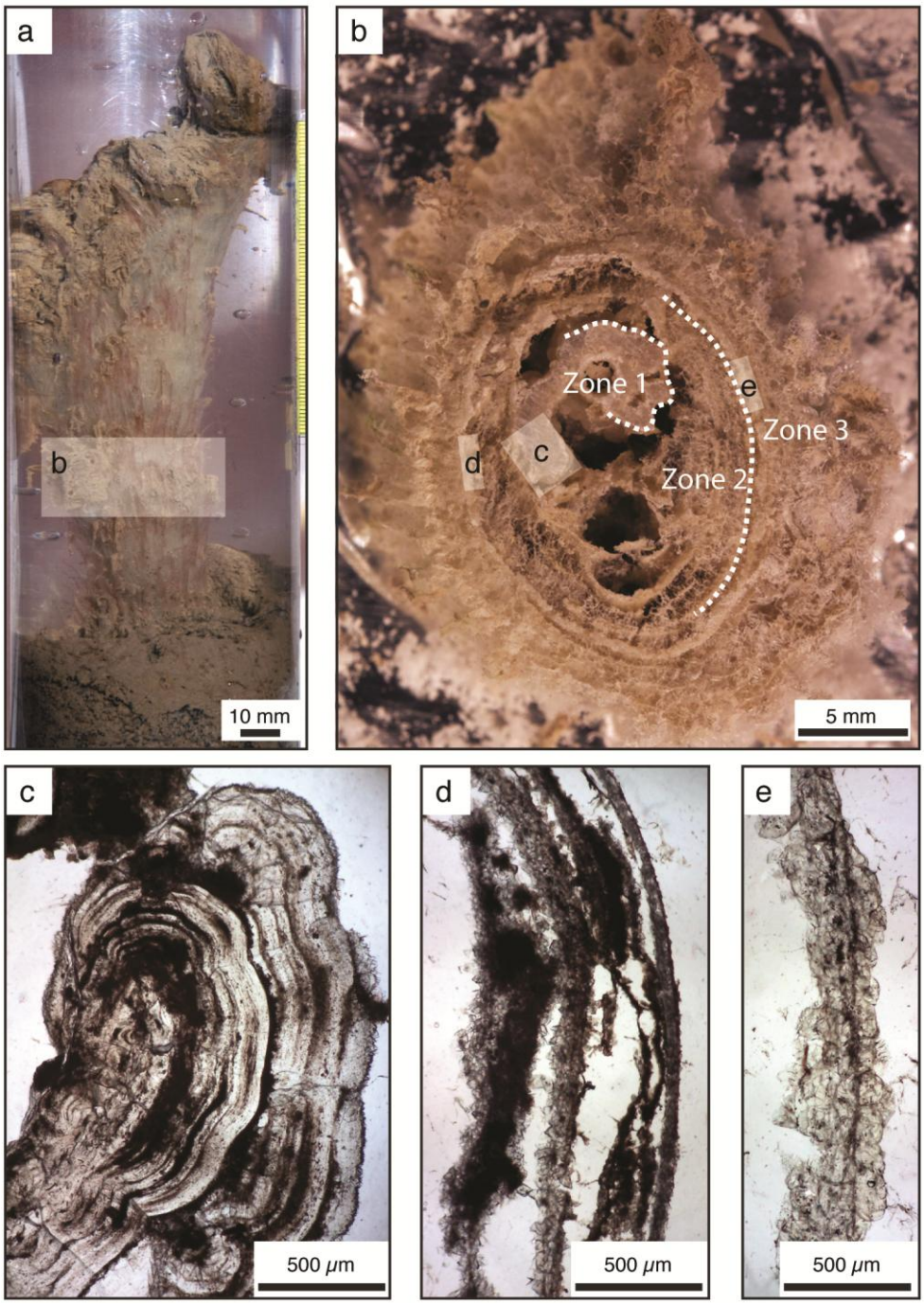
a
b
10 mm
b
Zone 1
e
Zone 3
d
c
Zone 2
5 mm
c
500 μm
d
500 μm
e
500 μm

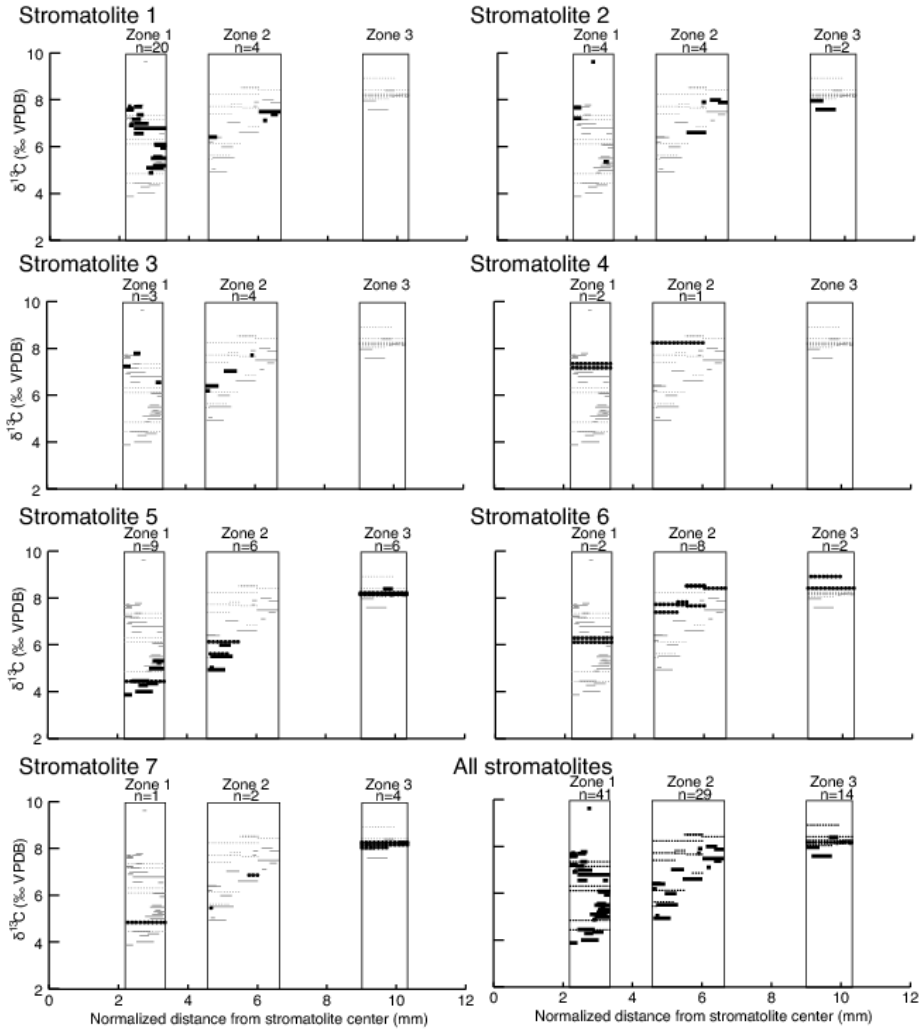
Stromatolite 1
Zone 1 n=20
Zone 2 n=4
Zone 3
Stromatolite 2
Zone 1 n=4
Zone 2 n=4
Zone 3 n=2
Stromatolite 3
Zone 1 n=3
Zone 2 n=4
Zone 3
Stromatolite 4
Zone 1 n=2
Zone 2 n=1
Zone 3
Stromatolite 5
Zone 1 n=9
Zone 2 n=6
Zone 3 n=6
Stromatolite 6
Zone 1 n=2
Zone 2 n=8
Zone 3 n=2
Stromatolite 7
Zone 1 n=1
Zone 2 n=2
Zone 3 n=4
All stromatolites
Zone 1 n=41
Zone 2 n=29
Zone 3 n=14
δ13C (‰ VPDB)
Normalized distance from stromatolite center (mm)

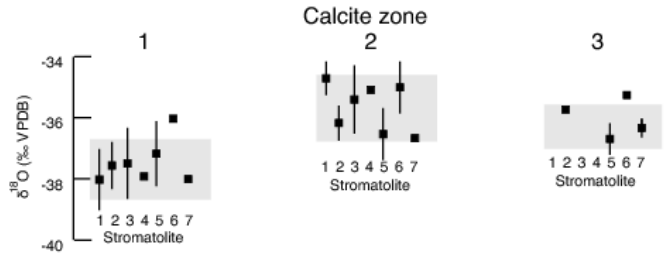
Calcite zone
1
2
3
-34
-36
-38
-40
$\delta^{18}O$ (‰ VPDB)
1 2 3 4 5 6 7
Stromatolite

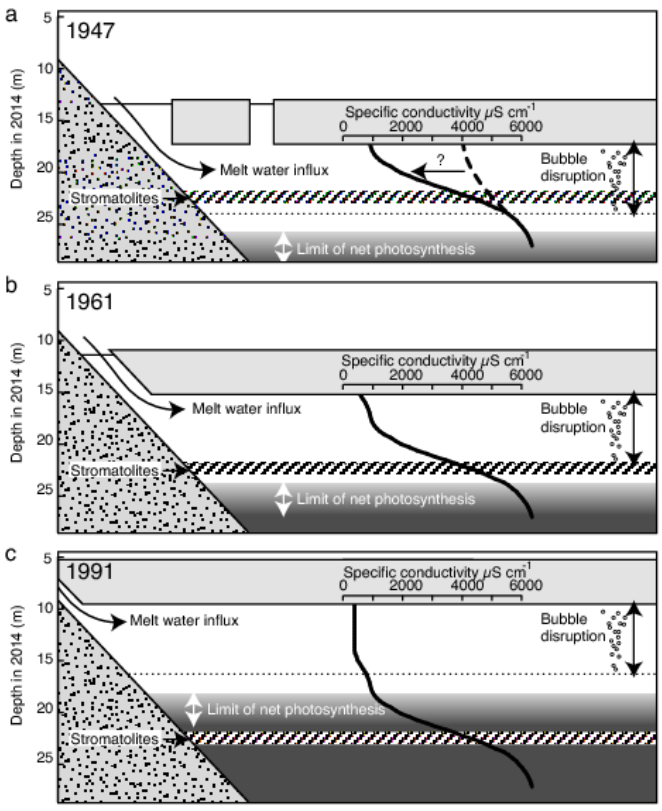
a
1947
Depth in 2014 (m)
5
10
15
20
25
Specific conductivity µS cm-1
0
2000
4000
6000
Melt water influx
?
Bubble disruption
Stromatolites
Limit of net photosynthesis
b
1961
Depth in 2014 (m)
Specific conductivity µS cm-1
0
2000
4000
6000
Melt water influx
Bubble disruption
Stromatolites
Limit of net photosynthesis
c
1991
Depth in 2014 (m)
Specific conductivity µS cm-1
0
2000
4000
6000
Melt water influx
Bubble disruption
Limit of net photosynthesis
Stromatolites

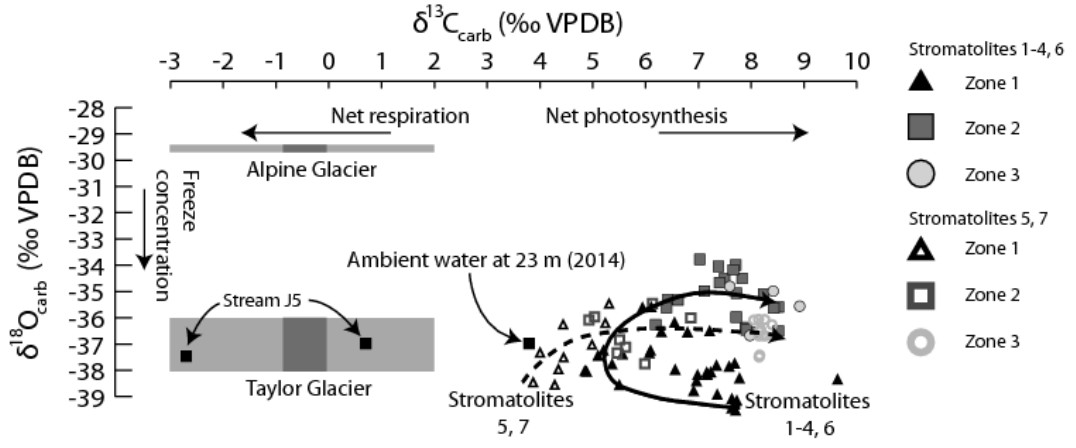
δ13Ccarb (‰ VPDB)
-3 -2 -1 0 1 2 3 4 5 6 7 8 9 10
δ18Ocarb (‰ VPDB)
-28 -29 -30 -31 -32 -33 -34 -35 -36 -37 -38 -39
Net respiration
Net photosynthesis
Alpine Glacier
Freeze concentration
Ambient water at 23 m (2014)
Stream J5
Taylor Glacier
Stromatolites 5, 7
Stromatolites 1-4, 6
Stromatolites 1-4, 6
Zone 1
Zone 2
Zone 3
Stromatolites 5, 7
Zone 1
Zone 2
Zone 3

Supplementary Materials

1. Supplemental methods

Water sample isotopic analysis

Water samples for $\delta^{13}C_{DIC}$ were prepared by injection of 5 mL water into 12 mL Exetainers containing 1 mL of 85% H_3PO_4 under He head space. Prepared Exetainers were analyzed at the UC Davis Stable Isotope Facility. Exetainers were flushed with a He carrier gas to pass sample CO_2 through a Poroplot Q GC column before entering a GasBench II interfaced to a Thermo Scientific Delta V Plus IRMS. Samples were run with 2 standards per 10 samples. Internal calibration standards had $\delta^{13}C$ values of +0.7 and -46.6‰, and secondary check standards had values of -2.4, -13.4 and -26.7‰. The long-term 1 σ analytical error on standards is ±0.1‰. Analysis of all water samples for $\delta^{18}O_{H20}$ was made on a Los Gatos Research, Inc. Laser Water Isotope Analyzer V2. Water samples were each injected 8 times, with the last four injections averaged for $^{18}O/^{16}O$ calculations. The internal check standard had a value of -28.6‰, and analytical 1 σ precision was 0.1‰ relative to the standard reference material. All $\delta^{18}O_{H20}$ values are reported relative to VSMOW.

Carbonate isotopic analysis

Powdered calcite samples from stromatolite layers were analyzed for $\delta^{13}C_{calcite}$ and $\delta^{18}O_{calcite}$ at the UC Davis Stable Isotope Lab. All samples were heated to 375 °C *in vacuo* for 30 minutes prior to analysis. 11 samples (Table S1) were reacted in individual sample containers with 105% H_3PO_4 in a Gilson Multicarb Autosampler and analyzed on a GV Instruments IsoPrime dual inlet mass spectrometer. These samples were run with an in-house Carrara Marble standard, UCD-SM92, for one point $\delta^{13}C$ and $\delta^{18}O$ standardization. The remaining 75 samples (Table S1) were analyzed on a GVI Optima Stable Isotope Ratio Mass Spectrometer with a common acid bath. Samples were run with NBS-18 and UCD-SM92 standards for independent one point correction for $\delta^{13}C$ and $\delta^{18}O$. Typical 1 σ precision of $\delta^{13}C$ and $\delta^{18}O$ is 0.03‰ and 0.05‰, respectively, based on repeat analyses of standard reference materials. $\delta^{13}C_{calcite}$ and $\delta^{18}O_{calcite}$ values are reported relative to VPDB.

Biomass ^{13}C isotopic analysis

Acidified biomass samples (see methods in manuscript) were combusted at 1000 °C with silvered copper oxide and chromium oxide, and oxides were removed by passage over reduced copper at 650 °C.

The CO_2 was entrained in a He carrier gas and passed through a magnesium perchlorate water trap before entering the isotope ratio mass spectrometer through a Carbosieve GC column. Typical 1 σ precision is 0.2‰ relative to standard reference materials. $\delta^{13}C_{org}$ values are reported relative to VPDB.

2. Aqueous stable isotope geochemistry

Sources of melt water in the McMurdo Dry Valleys have a wide range of isotopic composition. Throughout the McMurdo Dry Valleys, local alpine glaciers have much higher $\delta^{18}O_{H2O}$ values than glaciers fed from the polar plateau (Matsubaya et al., 1979; Gooseff et al., 2006). Alpine glaciers throughout the McMurdo Dry Valleys have decreasing $\delta^{18}O_{H2O}$ values with increasing distance from the coast (Gooseff et al., 2006). In the vicinity of Lake Joyce, ice sampled from the alpine Rhone Glacier has $\delta^{18}O_{H2O}$ values reported from -33.6‰ (Matsubaya et al., 1979) to -33.9‰ (Stuiver et al., 1981) for glacier ice. This is the closest alpine glacier to Lake Joyce that has been sampled for isotopic analysis. The ice-sheet derived Taylor glacier abutting Lake Joyce has reported $\delta^{18}O_{H2O}$ values of -42.5‰ (Matsubaya et al., 1979), -40.6‰ (Stuiver et al., 1981) and -40.4±2.3‰ (Gooseff et al., 2006) for glacier ice. Meltwater from both Taylor Glacier and alpine glaciers flow into Lake Joyce, where their isotopic compositions are mixed and further modified. $\delta^{18}O_{H2O}$ values for streams associated with glaciers throughout the McMurdo Dry Valleys are modified through flow by both evaporation and mixing with hyporheic fluids (Gooseff et al., 2003; Gooseff et al., 2006). Within lakes, freezing to the underside of the ice cover preferentially incorporates ^{18}O over ^{16}O (Horita, 2009; Lacelle, 2011), with maximum expected fractionation of approximately +3‰ into ice (O'Neil, 1968; Suzuoki and Kimura, 1973).

Unlike $\delta^{18}O_{H2O}$ values in streams, $\delta^{13}C_{DIC}$ values do not primarily correspond to the glacier source. Rather, $\delta^{13}C_{DIC}$ values vary from -9.4‰ to +5.1‰ in Taylor Valley lakes, with most between -3‰ and +2‰; flow-weighted average annual stream $\delta^{13}C_{DIC}$ values span a narrower range from -0.86‰ to -0.04‰ (Neumann, 1999; Neumann et al., 2004; Lyons et al., 2013). Flow-weighted averages were calculated from stream $\delta^{13}C_{DIC}$ values combined with stream flow measured at weirs (Neumann, 1999; Neumann et al., 2004). Stream $\delta^{13}C_{DIC}$ values are a product of both microbial processes and variable atmospheric equilibration (Neumann, 1999; Lyons et al., 2013). Changes in atmospheric $\delta^{13}C_{CO2}$ values due to anthropogenic release (e.g. Verburg, 2007) could lead to subtle long-term evolution of inflowing stream

DIC $^{13}C/^{12}C$ ratios due to the Suess effect, but the magnitude of these changes would likely be small compared to other isotope effects in the McMurdo Dry Valleys.

$\delta^{13}C_{DIC}$ values have been stable in most lakes over the course of a decade through both warm flood years with large influx of meltwater and cold years with little meltwater influx (Knoepfle et al., 2009). Perennial ice cover limits equilibration of DIC with atmospheric CO_2, and long-term evolution of $\delta^{13}C_{DIC}$ values can be significantly influenced by net oxygenic photosynthesis or respiration (Wharton et al., 1993; Neumann et al., 2001; Neumann et al., 2004; Knoepfle et al., 2009), with minor contributions by methane cycling in some lakes (Knoepfle et al., 2009). Deep waters below density stratified intervals typically have $\delta^{13}C_{DIC}$ values and DIC concentrations representing historical legacies of net respiration and freeze-concentration or evaporation (Neumann et al., 2004; Knoepfle et al., 2009). In contrast to legacy $\delta^{13}C_{DIC}$ values of saline deep waters, shallow waters comprising the freshwater lens in most lakes of the McMurdo Dry Valleys have $\delta^{13}C_{DIC}$ values reflecting modern net microbial activity (Neumann et al., 2001; Neumann et al., 2004; Knoepfle et al., 2009). Shallow water $\delta^{13}C_{DIC}$ values are not significantly affected by inflowing stream $\delta^{13}C_{DIC}$ values due to low stream DIC concentrations (Knoepfle et al., 2009). CO_{2aq} concentrations do vary seasonally, however, with measurable uptake in both Lake Fryxell (9% CO_{2aq}) and Lake Hoare (64% CO_{2aq}) interpreted as seasonal variations in photosynthesis (Neumann et al., 1998). In the high pH shallow water of most McMurdo Dry Valley lakes, CO_{2aq} is undersaturated due to lack of equilibration across the perennial ice cover (Andersen et al., 1998; Neumann et al., 2001).

3. Stromatolite mineralization and calcite isotopic composition

3.1. Timing of mineralization

Carbonate precipitation within Lake Joyce stromatolites preserves photosynthetic signatures. Variable and enriched $\delta^{13}C_{calcite}$ values have a local maximum in zones with the greatest expected photosynthetic rates (Fig. S3). pH gradients observed in actively growing photosynthetic mats indicate that rates of microbial activity may have been sufficient to generate photosynthetic isotopic signatures (see manuscript discussion section 5.1.3). Although these signatures support calcite precipitation during austral summer periods of photosynthetic activity, they do not exclusively restrict precipitation to the austral summer. Possible photosynthetic effects on DIC $^{13}C/^{12}C$ ratio can exceed the range observed in the Lake

Joyce stromatolites (Sumner, 2001), suggesting that calcite did not exclusively precipitate during times of peak photosynthesis. Mixing of phototrophic and heterotrophic signatures can lead to variable $\delta^{13}C_{calcite}$ values (e.g. Andres et al., 2006; Brady et al., 2013), and heterogeneous $\delta^{13}C_{calcite}$ values within individual stromatolite layers support variable photosynthetic influences on calcite precipitation. Calcite contains mud-rich laminae representing sediment that settled out of suspension following austral summer meltwater influx (Fig. 3), but it is not possible to resolve whether carbonate precipitation was synchronous with sedimentation or precipitation incorporated laminae in the mat subsurface. Within zone 1, carbonate botryoids were at least sufficiently close to the mat surface to affect patterns of lamina sedimentation, with the underside of botryoids sheltered from sediment accumulation (Mackey et al., 2015, Fig. 3). Similarly, carbonate entombed cyanobacteria filaments in a variety of orientations, with laminae of filaments perpendicular to the growth surface alternating with layers of filaments parallel to the growth surface (data not shown). These orientations are similar to seasonal laminae in benthic mats from elsewhere in the McMurdo Dry Valleys lacking carbonate precipitation (Hawes et al., 2001), and imply that carbonate either precipitated continuously through mat accumulation or at least did not disrupt lamination in the process of mineralization. Thus, carbonate could have precipitated over winter, but petrographic evidence does not require winter precipitation.

3.2. Photosynthetic controls on $\delta^{13}C_{calcite}$

As described in the manuscript discussion, trends in $\delta^{13}C_{calcite}$ values through stromatolite growth are most consistent with variable influence of primary productivity in zone 1, transitioning to long term modification of the ambient DIC pool $\delta^{13}C$ values by net photosynthesis. Across this period of stromatolite growth, other factors like meltwater influx and microbial community composition were also changing but did not likely exert a strong control on stromatolite $\delta^{13}C_{calcite}$ (see manuscript discussion for impact of meltwater on $\delta^{18}O_{H2O}$). Stream $\delta^{13}C_{DIC}$ values could have been 1-2‰ higher than recent measurements prior to significant anthropogenic release of ^{13}C-depleted CO_2 (Verburg, 2007). This possible long-term trend is unlikely to have had a significant impact on lake $\delta^{13}C_{DIC}$ values on the time scale of stromatolite growth. DIC concentrations of stream water are approximately 10× lower than concentrations at the depth of stromatolite growth (Neumann et al., 2004), reducing the potential for a large influence on ambient $\delta^{13}C_{DIC}$ values (Knoepfle et al., 2004). In general, meltwater influx through lake level rise also correlates to more

enriched stromatolite $\delta^{13}C_{calcite}$ values, despite the fact that inflowing meltwater would have had lower $\delta^{13}C_{DIC}$ values than expected for equilibrium precipitation with stromatolites (Fig. 7). Thus, trends in stromatolite $\delta^{13}C_{calcite}$ values are not consistent with meltwater influence. Changes in microbial community composition is also unlikely to have been a significant contributor to the changing stromatolite $\delta^{13}C_{calcite}$. The primary change in stromatolite $\delta^{13}C_{calcite}$ is between zone 1 and 2, whereas evidence for cyanobacterial community change from microfossils has the largest change between zone 2 and 3 (Mackey et al., 2015). Fractionation factors could be influenced by changes in carbon limitation, however. In other MDV lakes, decreased photosynthetic rates with depth lead to increasing fractionation between DIC and calcite (Lawson et al., 2004). Changes in DIC concentrations with fresh water influx and establishment of the pycnocline (see discussion) could have led to changes in the fractionation factor due to changes in the ratio between photosynthetic rates and available carbon. Increasing fractionation factors are not likely the sole cause of long term changes in stromatolite $\delta^{13}C_{calcite}$ values, however, as values remain consistently enriched in the outermost calcite as irradiance fell below the light limit for net photosynthesis.

The different patterns of $\delta^{13}C_{calcite}$ trends in stromatolites are more consistent with lateral heterogeneity in conditions controlling photosynthetic signatures (see manuscript discussion) than variations in the depths range of stromatolites sampled. Stromatolites were collected over a depth range of <2 m (Table 1). Given the extinction coefficient for irradiance in Lake Joyce (Hawes et al., 2011), the change in irradiance over the depth range of stromatolites would be ≈20%. Lateral variability in irradiance, in contrast, varies by >5-fold. Likewise, changes in DIC concentration with depth were likely insufficient to modulate microbial signatures preserved in $\delta^{13}C_{calcite}$ values; DIC concentrations in 2001 were calculated to vary from 1.3 to 1.7 mM over the depth range of stromatolites (Shacat et al., 2004). Thus, diverse local processes within the photosynthesizing mats where calcite zone 1 precipitated were probably the most important factors in controlling $\delta^{13}C_{calcite}$ values.

Mechanisms for local control on stromatolite carbonate isotopic composition could be directly or indirectly affected by microbial activity. In addition to the effects of photosynthetic DIC uptake and fractionation of the ambient $\delta^{13}C_{DIC}$ pool as described in the manuscript discussion, changes in calcite saturation state or pH could also affect the final calcite $\delta^{13}C$ and $\delta^{18}O$. Changes in saturation state from variability in pH/CO_3^{2-} concentration with microbial activity can affect $^{18}O/^{16}O$ fractionation between H_2O

and calcite, particularly given the cold water environment of Lake Joyce. Low temperature precipitation experiments have found $\varepsilon_{calcite\text{-}H2O}$ varying by 4‰ at a consistent 5°C and pH 9 with changing precipitation rate (Dietzel et al., 2009). Changing pH can further affect $^{18}O/^{16}O$ and $^{13}C/^{12}C$ fractionation (e.g. Spero et al., 1997; Zeebe, 1999) The small changes in pH with photosynthesis in Lake Joyce mats (pH 10.5-10.7) is unlikely to explain the large variability seen in calcite isotopic composition. Larger changes are possible, albeit unmeasured, with seasonal variations in photosynthesis and respiration rates (e.g. Moorhead et al., 2005), but there is no evidence for changes in relative contribution of austral summer versus winter precipitation among stromatolites or through stromatolite growth.

3.3. Temperature controls on $\delta^{18}O_{calcite}$ values

Temperature variability is not likely to have significantly affected stromatolite $\delta^{18}O_{calcite}$ values. Temperature in Lake Joyce is largely moderated by contact with Taylor Glacier (Spigel and Priscu, 1998), and the thick ice cover prevents significant solar heating as observed in Lake Vanda (e.g. Wilson and Wellman, 1962; Castendyk et al., 2016). Maximum temperatures of 1.1 °C recorded recently in Lake Joyce (Shacat et al., 2004) are most consistent with early measurements in 1972 (Hendy et al., 1973; Gumbly, 1975), though there is one report of maximum temperatures up to 2.5 °C (Parker et al., 1982). Nevertheless, the change of approximately +2‰ in $\delta^{18}O_{calcite}$ values through stromatolite growth would require an unreasonably large reduction of approximately 9 °C in temperature through time in Lake Joyce (Kim and O'Neil, 1997).

4. Supplemental figures and tables

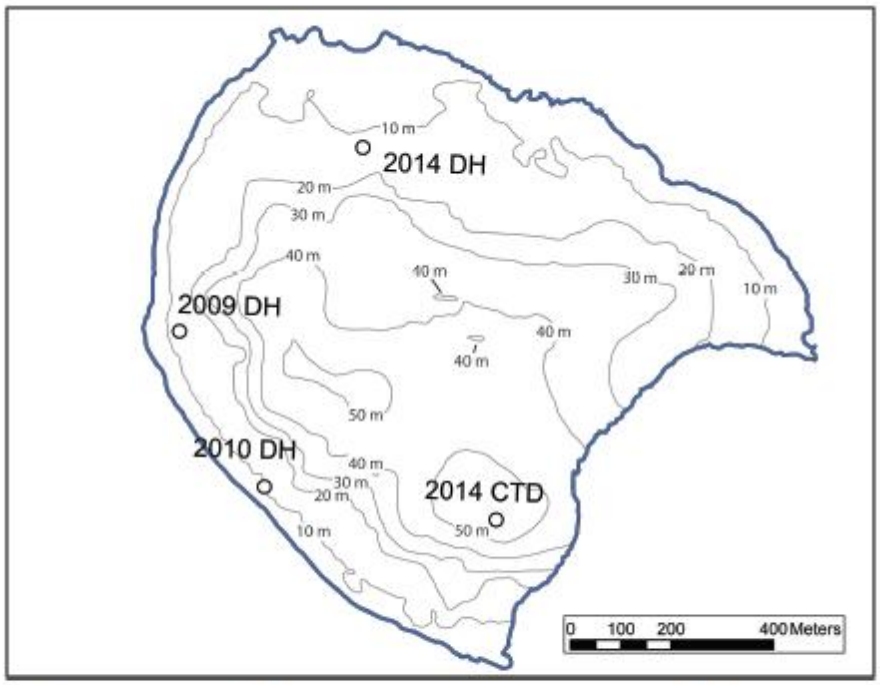

Fig. S1: Bathymetric map of Lake Joyce from depth soundings and orthorectified aerial photographs. Locations of dive sites are superimposed for 2009, 2010, and 2014. Water column sampling took place at the 2014 CTD site.

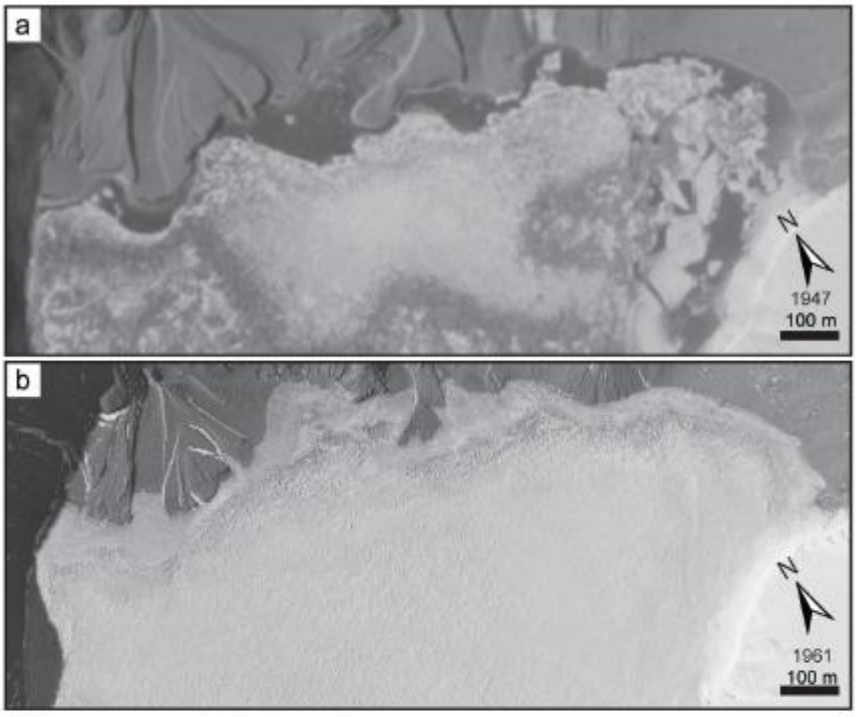

Fig. S2: Aerial photographs from 1947 (A) and 1961 (B) show the changing shoreline on the eastern side of Lake Joyce with lake level rise, including extensive fragmentation of the ice cover in 1947 (A).

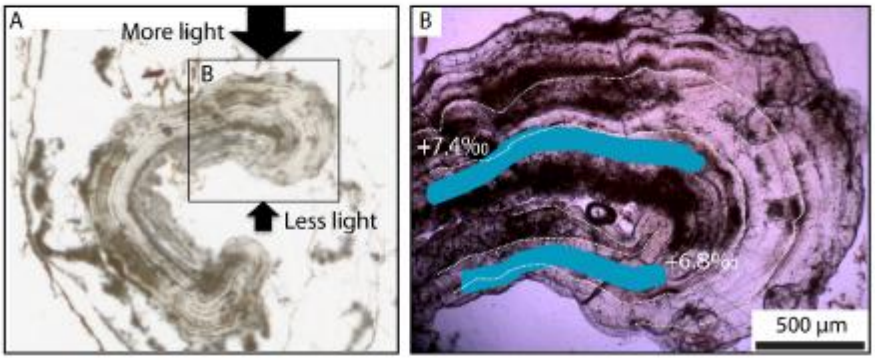

Fig. S3: Thin section cut from horizontal slice through stromatolite 1. Calcite of zone 1 (A) nucleated on a curved surface interpreted as bubble-supported liftoff mat. Acicular calcite was thickest on the outside of this curved surface and thinned toward the inside. Laminae can be traced around this surface, demonstrating that coeval calcite layers varied in thickness through growth. Thicker layers also have higher $\delta^{13}C_{calcite}$ values (B), consistent with the interpretation of photosynthetic enhancement of carbonate precipitation.

Table S1: Summary of carbonate isotopic data collected from all stromatolites in the course of this study. For details of methods used in Optima or Isoprime Multicarb, see Suppemental Materials section 1.

Stromatolite	$\delta^{13}C_{calcite}$	$\delta^{18}O_{calcite}$	Calcite zone	Instrument
1	7.71	-39.51	1	Optima
1	6.56	-37.96	1	Optima
1	6.99	-38.16	1	Optima
1	5.50	-38.54	1	Optima
1	6.09	-37.22	1	Optima
1	6.07	-37.32	1	Optima
1	7.63	-39.42	1	Optima
1	5.20	-37.22	1	Optima
1	7.73	-39.13	1	Optima
1	7.64	-39.06	1	Optima
1	5.10	-37.42	1	Optima
1	6.91	-38.76	1	Optima
1	7.17	-38.14	1	Optima
1	6.96	-38.38	1	Optima
1	5.56	-37.36	1	Optima
1	4.88	-38.02	1	Optima
1	7.36	-38.90	1	Optima
1	5.94	-35.59	1	Optima
1	7.58	-37.84	1	Optima
1	6.79	-36.53	1	Optima
2	5.37	-37.75	1	Optima
2	9.64	-38.32	1	Optima
2	7.21	-36.49	1	Optima
2	7.69	-37.72	1	Optima
3	7.78	-38.28	1	Optima
3	7.23	-38.05	1	Optima
3	6.55	-36.17	1	Optima
4	7.34	-37.79	1	Optima
4	7.16	-38.06	1	Optima
6	6.30	-36.52	1	Optima
6	6.11	-35.57	1	Optima
5	4.44	-36.23	1	IsoPrime Multicarb

5	4.00	-37.30	1	Optima
5	4.45	-37.49	1	Optima
5	4.99	-37.00	1	Optima
5	5.24	-36.18	1	Optima
5	4.35	-37.94	1	Optima
5	4.28	-38.53	1	Optima
5	5.31	-35.44	1	Optima
5	3.87	-38.44	1	Optima
7	4.85	-38.01	1	IsoPrime Multicarb
1	6.42	-35.31	2	Optima
1	7.50	-34.51	2	Optima
1	7.12	-34.98	2	Optima
1	7.38	-34.05	2	Optima
2	8.01	-36.56	2	Optima
2	7.89	-36.37	2	Optima
2	7.91	-36.46	2	Optima
2	6.61	-35.32	2	Optima
3	6.19	-36.26	2	Optima
3	6.40	-35.62	2	Optima
3	7.02	-33.78	2	Optima
3	7.72	-35.97	2	Optima
4	8.23	-35.10	2	Optima
6	7.71	-33.99	2	Optima
6	7.83	-34.50	2	Optima
6	8.52	-36.50	2	Optima
6	8.52	-35.59	2	Optima
6	7.66	-34.18	2	Optima
6	8.43	-35.62	2	Optima
6	7.72	-35.06	2	Optima
6	7.40	-34.66	2	Optima
5	5.62	-37.12	2	IsoPrime Multicarb
5	6.13	-35.46	2	IsoPrime Multicarb
5	5.51	-36.84	2	Optima
5	4.93	-36.08	2	Optima
5	5.03	-35.96	2	Optima
5	5.99	-37.75	2	Optima
7	5.46	-37.34	2	IsoPrime Multicarb
7	6.86	-36.00	2	Optima
2	7.98	-36.67	3	Optima
2	7.60	-34.80	3	Optima
6	8.92	-35.56	3	Optima
6	8.42	-34.98	3	Optima
5	8.22	-36.67	3	IsoPrime Multicarb
5	8.16	-37.42	3	IsoPrime Multicarb
5	8.15	-37.49	3	IsoPrime Multicarb
5	8.16	-36.51	3	IsoPrime Multicarb
5	8.15	-36.69	3	Optima
5	8.18	-36.44	3	Optima
5	8.14	-36.06	3	Optima

5	8.39	-36.26	3	Optima
7	8.16	-36.51	3	IsoPrime Multicarb
7	8.27	-36.69	3	IsoPrime Multicarb
7	8.26	-36.07	3	Optima
7	8.05	-36.09	3	Optima

5. Supplemental references

Andersen DT, McKay CP, Wharton RA (1998) Dissolved gases in perennially ice-covered lakes of the McMurdo Dry Valleys, Antarctica. Antarctic Science, 10, 124-133.

Andres MS, Sumner DY, Reid RP, Swart PK (2006) Isotopic fingerprints of microbial respiration in aragonite from Bahamian stromatolites. Geology, 34, 973-976. doi: 10.1016/j.sedgeo.2005.12.020

Brady AL, Druschel G, Leoni L, Lim DSS, Slater G (2013) Isotopic biosignatures in carbonate-rich, cyanobacteria-dominated microbial mats of the Cariboo Plateau, B.C. Geobiology, 11, 437-456. doi: 10.1111/gbi.12050

Castendyk DN, Obryk MK, Leidman SZ, Gooseff M, Hawes I (2016) Lake Vanda: A sentinel for climate change in the McMurdo Sound Region of Antarctica. Global and Planetary Change, 144, 213-227. doi: 10.1016/j.gloplacha.2016.06.007

Gooseff MN, McKnight DM, Runkel RL, Vaught BH (2003) Determining long time-scale hyporheic zone flow paths in Antarctic streams. Hydrological Processes, 17, 1691-1710

Gooseff MN, Lyons W, McKnight DM, Vaughn BH, Fountain AG, Dowling C (2006) A stable isotopic investigation of a polar desert hydrologic system, McMurdo dry valleys, Antarctica. Arctic, Antarctic And Alpine Research, 38, 60-71.

Gumbley JW (1975) A sedimentological study of three saline lakes in the Dry Valleys of Victoria Land, Antarctica. In: Earth Science Department. University of Waikato.

Hawes I, Moorhead D, Sutherland D, Schmeling J, Schwarz AM (2001) Benthic primary production in two perennially ice-covered Antarctic lakes: patterns of biomass accumulation with a model of community metabolism. Antarctic Science, 13, 18-27.

Hawes I, Sumner DY, Andersen DT, Mackey TJ (2011) Legacies of recent environmental change in the benthic communities of Lake Joyce, a perennially ice-covered Antarctic lake. Geobiology, 9, 394-410. doi: 10.1111/j.1472-4669.2011.00289.x

Hendy CH, Hogg AG, Hosking PL, Oliver TI (1973) Antarctic Research Unit Report no. 3. University of Waikato, pp. 6.

Horita J (2009) Isotopic evolution of saline lakes in the low-latitude and polar regions. Aquatic Geochemistry, 15, 43-69. doi: 10.1007/s10498-008-9050-3

Kim ST, O'Neil JR (1997) Equilibrium and nonequilibrium oxygen isotope effects in synthetic carbonates. Geochimica et Cosmochimica Acta, 61, 3461-3475.

Knoepfle JL, Doran PT, Kenig F, Lyons WB, Galchenko VF (2009) Particulate organic and dissolved inorganic carbon stable isotopic compositions in Taylor Valley lakes, Antarctica: the effect of legacy. Hydrobiologia, 632, 139-156. doi: 10.1007/s10750-009-9834-5

Lacelle D (2011) On the δ18O, δD, and D-excess Relations in Meteoric Precipitation and During Equilibrium Freezing: Theoretical Approach and Field Examples. Permafrost and Periglacial Processes, 22, 13-25. doi: 10.1002/ppp.712

Lyons WB, Leslie DL, Harmon RS, Neumann K, Welch KA, Bisson KM, McKnight DM (2013) The carbon stable isotope biogeochemistry of streams, Taylor Valley, Antarctica. Applied Geochemistry, 32, 26-36. doi: 10.1016/j.apgeochem.2012.08.019

Mackey TJ, Sumner DY, Hawes I, Jungblut AD, Andersen DT (2015) Growth of modern branched columnar stromatolites in Lake Joyce, Antarctica. Geobiology, 13, 373-390. doi: 10.1111/gbi.12138

Matsubaya O, Sakai H, Torii T, Burton H, Kerry K (1979) Antarctic saline lakes -- stable isotopic ratios, chemical compositions and evolution. Geochimica et Cosmochimica Acta, 43, 7-25. doi: 10.1016/0016-7037(79)90042-5

Moorhead D, Schmeling J, Hawes I (2005) Modelling the contribution of benthic microbial mats to net primary production in Lake Hoare, McMurdo Dry Valleys. Antarctic Science, 17, 33-45. doi: 10.1017/S0954102005002403

Neumann K, Lyons WB, Des Marais DJ (1998) Inorganic carbon-isotope distribution and budget in the Lake Hoare and Lake Fryxell basins, Taylor Valley, Antarctica. Annals of Glaciology, 27, 685-690.

Neumann K (1999) Carbon dynamics in lakes and streams of Taylor Valley, Antarctica. University of Alabama.

Neumann K, Lyons WB, Priscu JC, Donahoe RJ (2001) CO_2 concentrations in perennially ice-covered lakes of Taylor Valley, Antarctica. Biogeochemistry, 56, 27-50.

Neumann K, Lyons WB, Priscu JC, DesMarais DJ, Welch KA (2004) The carbon isotopic composition of dissolved inorganic carbon in perennially ice-covered Antarctic lakes: searching for a biogenic signature. Annals of Glaciology, 39, 518-524. doi: 10.3189/172756404781814465

O'Neil JR (1968) Hydrogen and Oxygen Isotope Fractionation between Ice and Water. Journal of Physical Chemistry, 72, 3683-3684.

Parker BC, Simmons GM, Seaburg KG, Cathey DD, Allnutt FCT (1982) Comparative ecology of plankton communities in seven Antarctic oasis lakes. Journal of Plankton Research, 4, 271-286.

Shacat JA, Green WJ, DeCarlo EH, Newell S (2004) The Geochemistry of Lake Joyce, McMurdo Dry Valleys, Antarctica. Aquatic Geochemistry, 10, 325-352. doi: 10.1023/B:AQUA.0000047184.50027.41

Spero HJ, Bijma J, Lea DW, Bemis BE (1997) Effect of seawater carbonate concentration on foraminiferal carbon and oxygen isotopes. Nature, 390, 497-500. doi: 10.1038/37333

Spigel RH, Priscu JC (1998) Physical Limnology of the McMurdo Dry Valleys Lakes. In: Ecosystem Dynamics in a Polar Desert: the McMurdo Dry Valleys, Antarctica (ed Priscu JC). American Geophysical Union, Washington, DC.

Stuiver et al., 1981

Sumner DY (2001) Microbial Influences on Local Carbon Isotopic Ratios and Their Preservation in Carbonate. Astrobiology, 1, 57-70. doi: 10.1089/153110701750137431

Suzuoki T, Kimura T (1973) D/H and 18O/16O Fractionation in Ice-Water system. Mass Spectroscopy, 21, 229-233. doi: 10.5702/massspec1953.21.229

Verburg P (2007) The need to correct for the Suess effect in the application of d13C in sediment of autotrophic Lake Tanganyika, as a productivity proxy in the Antropocene. Journal of Paleolimnology, 37, 591-602.

Wilson AT, Wellman HW (1962) Lake Vanda: An Antarctic Lake. Nature, 4860, 1171-1173.

Zeebe RE (1999) An explanation of the effect of seawater carbonate concentration on foraminiferal oxygen isotopes. Geochimica et Cosmochimica Acta, 63, 2001-2007. doi: 10.1016/S0016-7037(99)00091-5